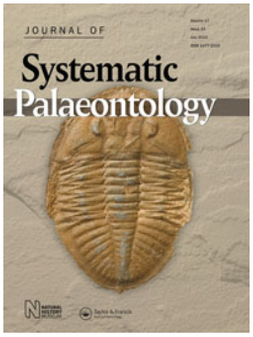

Taylor & Francis
Taylor & Francis Group

Journal of Systematic Palaeontology

ISSN: 1477-2019 (Print) 1478-0941 (Online) Journal homepage: https://www.tandfonline.com/loi/tjsp20

Revision of *Undorosaurus*, a mysterious Late Jurassic ichthyosaur of the Boreal Realm

Nikolay G. Zverkov & Vladimir M. Efimov

To cite this article: Nikolay G. Zverkov & Vladimir M. Efimov (2019) Revision of *Undorosaurus*, a mysterious Late Jurassic ichthyosaur of the Boreal Realm, Journal of Systematic Palaeontology, 17:14, 963-993, DOI: 10.1080/14772019.2018.1515793

To link to this article: https://doi.org/10.1080/14772019.2018.1515793

Journal of Systematic Palaeontology, 2019
Vol. 17, No. 14, 963–993, http://dx.doi.org/10.1080/14772019.2018.1515793

Revision of *Undorosaurus*, a mysterious Late Jurassic ichthyosaur of the Boreal Realm

Nikolay G. Zverkov[a,b,c]* and Vladimir M. Efimov[d]

[a]*Geological Faculty, Lomonosov Moscow State University, Leninskie Gory 1, Moscow 119991, Russia;* [b]*Geological Institute of the Russian Academy of Sciences, Pyzhevsky Lane 7, Moscow 119017, Russia;* [c]*Borissiak Paleontological Institute of the Russian Academy of Sciences, Profsoyuznaya St., 123, Moscow 117997, Russia;* [d]*Undory Paleontological Museum, Village of Undory, Ulyanovsk Region 433312, Russia*

(Received 2 December 2017; accepted 10 August 2018)

Recent study of ophthalmosaurid ichthyosaurs has brought us a number of new taxa; however, the validity of several ophthalmosaurid taxa from the Volgian (Tithonian) of European Russia still remains unclear, complicating comparisons and in some cases affecting taxonomic decisions about new contributions. A revision of the type series of all three species of *Undorosaurus*, erected by Efimov in 1999, reveals the potential validity of two of them. This contradicts previous research, which concluded that only the type species, *U. gorodischensis*, is valid. Furthermore, examination of the holotype of *Cryopterygius kristiansenae* from coeval strata of Svalbard shows that it is synonymous with *Undorosaurus gorodischensis*, sharing all diagnostic features of the species, especially those related to forelimb morphology: humerus with extensive anteroposteriorly elongate proximal end, poorly pronounced trochanter dorsalis and reduced deltopectoral crest; and ulna proximodistally elongate and not involved in perichondral ossification on its whole posterior edge. This supports the idea of intensive exchange of ichthyosaurs between the Middle Russian Sea and other Boreal seas in the Late Jurassic. In order to resolve the phylogenetic position of *Undorosaurus* within Ophthalmosauridae as well as relationships of other ophthalmosaurids, a new data set including 33 taxa and 106 characters, 23 of which are new, was compiled. The results of this analysis challenge all previous phylogenetic hypotheses for Ophthalmosauridae in a number of aspects, including the fact that *Undorosaurus* spp. was recovered deeply nested within Platypterygiinae as a sister group to derived platypterygiines.

Keywords: Ichthyosaurs; Ophthalmosauridae; *Undorosaurus*; Upper Jurassic; Volgian; Tithonian

Introduction

Ophthalmosauridae is a highly derived clade of ichthyosaurs that appeared in the Middle Jurassic (Fernández 1999, 2003; Druckenmiller & Maxwell 2014) and dominated until the extinction of ichthyosaurs in the early Late Cretaceous (Fischer *et al.* 2016). In the last decade, new ophthalmosaurid taxa have been erected from the Arctic (Maxwell 2010; Druckenmiller *et al.* 2012; Roberts *et al.* 2014; Delsett *et al.* 2017) and Europe (Tyborowski 2016; Paparella *et al.* 2017) that have illuminated the previously underestimated taxonomic diversity of Late Jurassic ichthyosaurs. This 'renaissance' in the study of Late Jurassic ichthyosaurs was preceded by a conservative period when their diversity was considered to be "on the low side" (Maisch & Matzke 2000, p. 90), and when Late Jurassic ichthyosaurs of the Northern Hemisphere were considered to be represented by only three genera: *Ophthalmosaurus*, and the much rarer *Brachypterygius* and *Nannopterygius* (Maisch & Matzke 2000).

Since 1997 several ophthalmosaurid taxa (three genera and 12 species) have been erected, based on materials from the Upper Jurassic (Volgian/Tithonian) of European Russia (Arkhangelsky 1997, 1998, 2001b; Efimov 1998, 1999a, b). These genera were soon regarded as subjective junior synonyms of *Ophthalmosaurus* and *Brachypterygius* (Maisch & Matzke 2000; McGowan & Motani 2003), although the validity of most of the Russian ichthyosaurs was questioned without first-hand examination (Maisch & Matzke 2000; Storrs *et al.* 2000; McGowan & Motani 2003; Maisch 2010). The first attempts to reassess some of these taxa have been undertaken only recently (Arkhangelsky & Zverkov 2014; Zverkov *et al.* 2015a). However, the type series of *Undorosaurus* has been awaiting a thorough required revision.

*Corresponding author. Email: zverkovnik@mail.ru

Published online 24 Jan 2019

Despite all of the debates on its validity and poorly understood osteology (see Maisch & Matzke 2000; McGowan & Motani 2003; Maisch 2010), *Undorosaurus* has frequently been used for comparative purposes when other Late Jurassic ophthalmosaurids are discussed (e.g. Maxwell 2010; Druckenmiller *et al.* 2012; Roberts *et al.* 2014; Delsett *et al.* 2017; Paparella *et al.* 2017). The phylogenetic position of *Undorosaurus* is no less controversial. First attempts to include *Undorosaurus* in a phylogenetic context were undertaken only 15 years after the taxon was described (Arkhangelsky & Zverkov 2014; Roberts *et al.* 2014). The position of *Undorosaurus* varied sufficiently in recovered phylogenies that the need for a redescription of the type material is clear. Therefore, some researchers have preferred to avoid including *Undorosaurus* in phylogenetic analyses (Fischer *et al.* 2016; Ji *et al.* 2016), whereas others have continued to consider this taxon, despite the absence of adequate data on its morphology (Maxwell *et al.* 2016; Delsett *et al.* 2017; Moon 2017; Paparella *et al.* 2017).

This paper is a part of an ongoing project on the taxonomy and phylogeny of the Late Jurassic ichthyosaurs of the Boreal Realm. The goals of this contribution are to redescribe the type material of *Undorosaurus*, and to assess the position of this genus in a modern taxonomic and phylogenetic framework.

Material and methods

The principal focus of this paper is the type material of *Undorosaurus gorodischensis*, *U. nessovi* and *U. khorlovensis*, stored in the Undory Palaeontological Museum, Ulyanovsk Region, Russia (UPM). Additionally, one of us (NGZ) has personally examined the holotype of *Cryopterygius kristiansenae* (PMO 214.578), which is on display in the Natural History Museum, University of Oslo, Norway.

Specimen UPM EP-II-20(572), the holotype of *Undorosaurus gorodischensis*, is a relatively complete, disarticulated skeleton, including most of the skull, 27 vertebrae, ribs, pectoral and pelvic girdles and limbs. It was collected from the bank of the Volga River near Gorodischi village, Ulyanovsk Province; Upper Jurassic, middle Volgian (Tithonian), *Epivirgatites nikitini* Ammonite Biozone.

UPM EP-II-23(744) is a fragmentary skeleton, with incomplete left mandibular ramus, stapes, several teeth, 36 vertebral centra including atlas-axis complex, rib fragments, fragmentary left coracoid and scapula, and incomplete left forelimb. It was collected from the bank of the Volga River near Gorodischi village, Ulyanovsk Province; Upper Jurassic, upper Volgian (Tithonian), *Garniericeras catenulatum* Ammonite Biozone.

UPM EP-II-21(1075) is an incomplete skeleton comprising fragments of the premaxilla and nasal, basioccipital, mandibular fragments, atlas-axis and 17 presacral vertebrae, fragments of the coracoids and scapulae, incomplete left forelimb and fragments of right forelimb. It was collected from the bank of the Volga River near Gorodischi village, Ulyanovsk Province; Upper Jurassic, middle Volgian (Tithonian), *Epivirgatites nikitini* Ammonite Biozone.

UPM EP-II-22(1073), an incomplete skeleton, comprises: fragmentary left nasal, left prefrontal, basioccipital, opisthotic, and stapes; complete left and partial right quadrates; mandibular fragments; hyoids; atlas-axis and 17 vertebrae; rib fragments; right coracoid and scapular fragments; incomplete humerus, radius and ulna; and autopodial elements. It was collected from the bank of the Volga River near Gorodischi village, Ulyanovsk Province; Upper Jurassic, middle Volgian (Tithonian), *Epivirgatites nikitini* Ammonite Biozone.

UPM EP-II-24(785), the holotype of *U. nessovi*, comprises a disarticulated skeleton, including basisphenoid, basioccipital (severely eroded), right stapes, quadrates, articular and surangular, hyoid, atlas-axis and 15 vertebrae, rib fragments, coracoid, scapulae, and nearly complete right and fragmentary left forelimbs. It was collected from the bank of the Volga River near Slantsevy Rudnik village, Ulyanovsk Province; Upper Jurassic, middle Volgian (Tithonian), *Virgatites virgatus* Ammonite Biozone.

UPM EP-II-27(870), the holotype of *U. khorlovensis*, comprises fragments of the snout, three vertebrae, incomplete scapulae, humeri, radius, and a femur fragment. It was collected at a phosphate mine near Khorlovo village, Voskresensk District, Moscow Province; Upper Jurassic, middle Volgian (Tithonian), *Virgatites virgatus* Ammonite Biozone.

YKM 44028-7 is an articulated left forelimb in matrix, collected from the bank of the Volga River near 'Detskiy sanatorium' Ulyanovsk Province; Upper Jurassic, middle Volgian (Tithonian), *Epivirgatites nikitini* Ammonite Biozone.

PMO 214.578, the holotype of *Cryopterygius kristiansenae*, is a nearly complete skeleton, from Svalbard, Norway; Upper Jurassic, middle Volgian (middle Tithonian), *Crendonites anguinus* Ammonite Biozone.

Comments on stratigraphy

Because of high faunal provincialism among marine invertebrates during the latest Jurassic and earliest

Cretaceous, independent regional marine stages are often used. In the so-called Pan-Boreal Superrealm, the Volgian and Ryazanian stages are used instead of the Tithonian and Berriasian international units. Although the bases of the Tithonian and Volgian stages are approximately contemporaneous (Rogov 2010a), their upper boundaries are not (Fig. 1). Recent contributions on this issue demonstrated that the Tithonian–Berriasian boundary can be traced in the Pan-Boreal Superrealm, where it corresponds to a horizon within the Boreal *Craspedites* (*Taimyroceras*) *taimyrensis* Ammonite Biozone that is upper Volgian (Houša *et al.* 2007; Bragin *et al.* 2013). This zone is nearly equivalent to the *C.* (*Trautscholdiceras*) *nodiger* Ammonite Biozone of the Russian Platform (Rogov & Zakharov 2009). In this regard, all the specimens described in this paper are Tithonian in age. Considering that most of the Upper Jurassic marine reptile localities of the Northern Hemisphere belong to the Pan-Boreal Superrealm and therefore ichthyosaurs from a number of formations in European Russia, Poland, England and Norway are from the Volgian or equivalents, we use both Volgian and Tithonian in this paper, with comments where necessary.

In European Russia, ichthyosaur remains referable to *Undorosaurus* have been found in the middle and upper Volgian (Fig. 1; *Virgatites virgatus*, *Epivirgatites nikitini* and *Garniericeras catenulatum* ammonite biozones). In Poland, specimen GMUL UŁ no. 3579-81, referred to here as *U. kielanae* comb. nov., originates from the middle Volgian *Zaraiskites scythicus* Ammonite Biozone (Fig. 1; Marţja & Wierzhbowski 2016; Tyborowski 2016). The stratigraphical position of specimens from Svalbard (including PMO 214.578) is imprecisely known, primarily due to insufficient control of reptile records by the ammonite succession (see Delsett *et al.* 2016). Originally Druckenmiller *et al.* (2012, p. 312) indicated that PMO 214.578 occurred in "either the *Dorsoplanites maximus* or the *D. ilovaiskyi* zone, corresponding to the Middle Volgian". However, the ammonites found in association with PMO 214.578 (see Supplemental Fig. S1) were identified by M. A. Rogov (GIN) as *Taimyrosphinctes evolutus* Mesezhnikov, 1984, known from the *Taimyrosphinctes excentricus* Ammonite Biozone of Siberia that corresponds to the *Crendonites anguinus* Ammonite Biozone of Svalbard (Fig. 1; Rogov 2010b).

Phylogenetic analysis

To test the phylogenetic position of *Undorosaurus* and other Late Jurassic ichthyosaurs, we analysed a modified version of the data set of Fischer *et al.* (2012; updated from Fischer *et al.* 2014a, b, 2016). Thirty-seven characters were added, including 23 new characters and 14 taken from previous studies by other authors (Motani 1999a; Sander 2000; Maxwell *et al.* 2012, 2016; Roberts *et al.* 2014; Zverkov *et al.* 2015a). Additionally, 13 characters were modified. A description of all characters is given in the Supplemental material. Seven operational taxonomic units (OTUs) were added to the matrix of Fischer *et al.* (2016), whereas most of the more basal parvipelvian OTUs included by Fischer *et al.* (2016), as well as characters applicable to them only, were not included in our analysis, as our principal focus was the relationships within Ophthalmosauridae. Taxa with high proportions of missing data (> 75%) were not included in our analysis; these are *Platypterygius sachicarum* (77%), *Muiscasaurus catheti* (77%), *Simbirskiasaurus birjukovi* (77%) and *Pervushovisaurus bannovkensis* (87%). Additionally, we critically revaluated some scores based on personal observations and the recent literature for *Arthropterygius chrisorum*, *Caypullisaurus bonapartei*, *Janusaurus lundi*, *Keilhauia nui*, *Maiaspondylus lindoei* and *Palvennia hoybergeti* (see Supplemental material 1). These changes resulted in a matrix of 33 taxa and 106 characters (see Supplemental material).

To analyse the taxon-character matrix we used TNT v. 1.5 (Goloboff & Catalano 2016), applying a traditional search with 10,000 replicates and tree bisection and reconnection (TBR) with 100 trees saved per replication. The RAM allocation was extended to 1024 megabytes (mxram 1024) and the memory to 50,000 trees. Decay indices (Bremer support, 'suboptimal' = 5) and resampling methods to estimate the robustness of nodes (standard bootstrapping and jackknifing, 1000 iterations) were also computed in TNT v. 1.5 (Goloboff & Catalano 2016). In our analysis we coded *Undorosaurus gorodischensis* (UPM EP-II-20(572)) and *Cryopterygius kristiansenae* (PMO 214.578) as a single unit with very high (90%) scoring. Additionally, we ran an analysis holding them as separate OTUs. The additional data set was analysed using the exact same procedures as described above.

Abbreviations

Anatomical abbreviations

aae, anterior accessory epipodial element; **acr**, acromial process; **ang**, angular; **ano**, anterior notch; **art.b**, articular boss; **at-ax**, atlas-axis complex; **con**, basioccipital condyle; **d2–d4**, distal carpals; **dp**, dorsal process of the femur; **dpc**, deltopectoral crest; **dpl**, dorsal plateau of

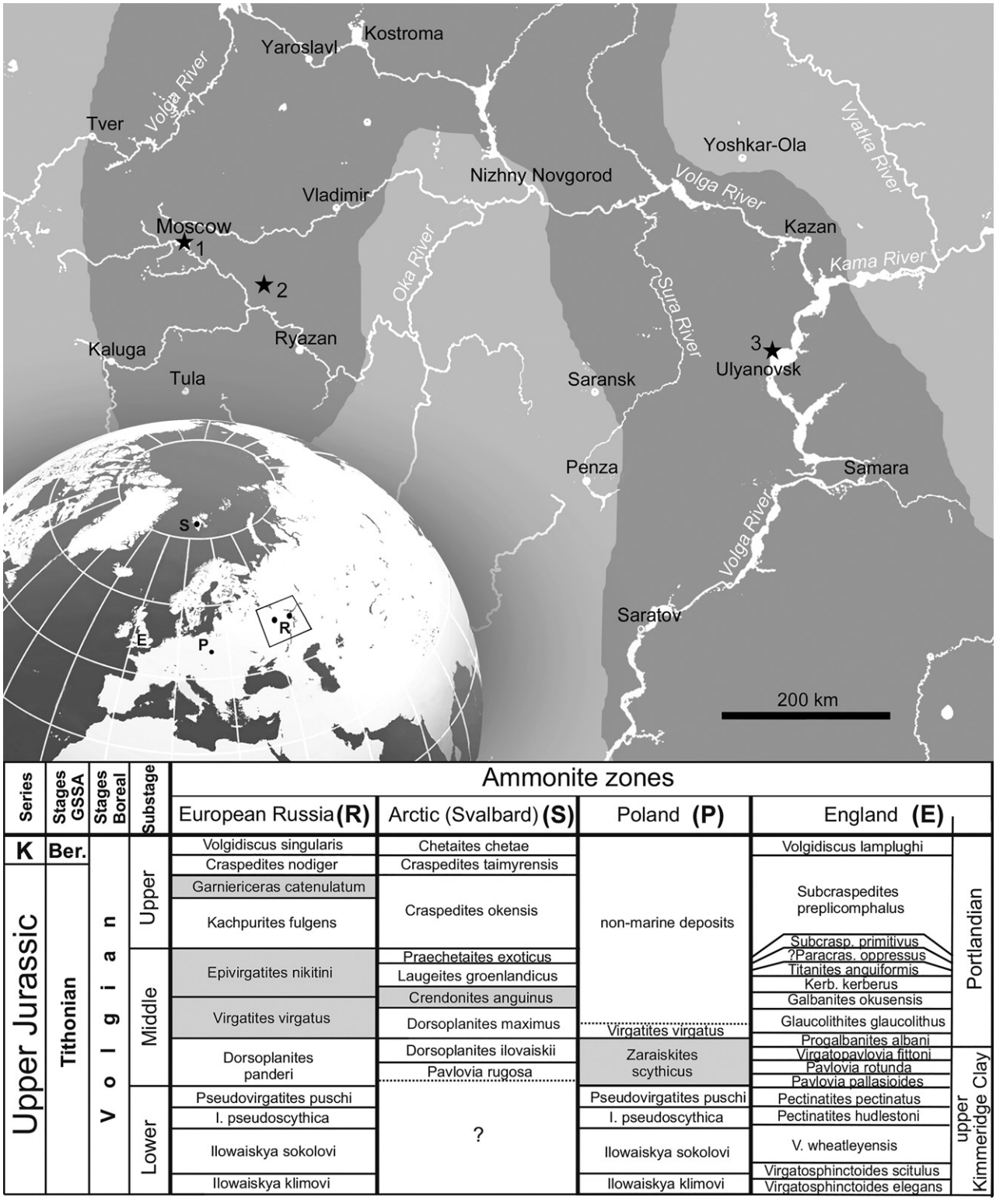

Figure 1. Maps showing the discovery sites of *Undorosaurus* specimens in European Russia and globally. Dark colour on the map of European Russia shows the area occupied by the Middle Russian Sea during the Volgian according to Sasonova & Sasonov (1967). Localities are marked with a star: 1, Moscow; 2, Lopatino phosphorite mine (Moscow Province); 3, bank of the Volga near Gorodischi village, Slantsevy Rudnik village and 'Detskiy sanatorium' (Ulyanovsk Province). Shown beneath is the zonal correlation of the Volgian regional stage of the European part of Russia, Spitsbergen, Poland and England. Distribution of *Undorosaurus* spp. is shown in grey. Correlation of ammonite zones after Rogov & Zakharov (2009), Rogov (2010b, 2017), Martja & Wierzbowski (2016) and Kiselev *et al.* (2018).

the basisphenoid; **eca**, extracondylar area; **exc**, *excavatio internasalis*; **faae**, facet for the anterior accessory element; **fan**, facet for the angular; **fbocc**, facet for the basioccipital; **fbs**, facet for the basisphenoid; **fco**, facet for the coracoid; **fep**, facet for the epipterygoid; **fex**, facet for the exoccipital; **fgl**, glenoid contribution of the scapula; **fi**, fibula; **fn**, facet of the neomorph; **fop**, facet for the opisthotic; **for**, foramina continuing the longitudinal groove; **fpi**, facet for the pisiform; **fpm**, facet for the premaxilla; **fpo**, facet for the postorbital and the jugal; **fpof**, facet for the postfrontal; **fpt**, facet for the pterygoid; **fq**, facet for the quadrate; **fr**, facet for the radius; **fsc**, facet for the scapula; **fso**, supraoccipital facet; **fst**, facet for the stapes; **fsut**, facet for the supratemporal; **fu**, facet for the ulna; **gr**, longitudinal groove located on the premaxilla and the dentary; **hy**, hyoid process; **i**, intermedium; **icf**, foramen for the internal carotid arteries; **ich**, impression of the cerebral hemisphere; **iop**, impression of the optic lobe; **isch**, ischium; **jug**, jugal; **lw**, lateral wing of the nasal lamella; **ma**, muscle (*M. adductor mandibulae externus*) attachment point; **mf**, medial facet; **mr**, muscular ridge on the opisthotic; **mx**, maxilla; **n**, neomorphic element; **na**, neural arch fragment; **nas**, nasal; **n.for**, supranarial foramen of the nasal housing blood vessels and/or nerves; **occl**, occipital lamella; **op**, opisthotic; **pcp**, paracoronoid process; **pi**, pisiform; **pm**, premaxilla; **pms**, posterior median stem; **poc**, paroccipital process; **pof**, postfrontal; **porb**, postorbital; **pref**, prefrontal; **proc.nar**, process narialis; **pu**, pubis; **q**, quadrate; **qj**, quadratojugal; **r**, radius; **ra**, radiale; **sof**, supraoccipital foramina; **sq**, squamosal; **sur**, surangular; **sur.b**, surangular boss;? **sut**, supratemporal fragment; **td**, *trochanter dorsalis*; **t**, tibiale; **ti**, tibia; **trab**, facets for cartilaginous continuation of the *cristae trabeculares*; **u**, ulna; **ul**, ulnare; **v3–4**, vertebrae with numbers; **vf**, vagus foramen; **VII**, groove of the facialis nerve (VII); **vp**, ventral process of the femur; **XII**, hypoglossal foramina.

Institutional abbreviations

GIN, Geological Institute of the Russian Academy of Sciences, Moscow, Russia; **GMUL**, Geological Museum of the University of Lodz, Poland; **MJML**, The Etches Collection, Museum of Jurassic Marine Life, Kimmeridge, Dorset, England; **NHMUK**, Natural History Museum, London, UK; **PMO**, Natural History Museum, University of Oslo (Palaeontological collection), Oslo, Norway; **SGM**, Vernadsky State Geological Museum of RAS, Moscow, Russia; **UPM**, Undory Palaeontological museum, Undory, Ulyanovsk Province, Russia; **YKM**, Ulyanovsk Regional Museum of Local Lore named after I. A. Goncharov, Ulyanovsk, Russia.

Data archiving statement

Data for this study are available in Morphobank: https://morphobank.org/permalink/?P2788

Systematic palaeontology

Ichthyosauria de Blainville, 1835
Ophthalmosauridae Baur, 1887
Platypterygiinae Arkhangelsky, 2001a *sensu* Fischer, Maisch, Naish, Kosma, Liston, Joger, Krüger, Pardo, Pérez, Tainsh & Appleby, 2012
Genus ***Undorosaurus*** Efimov, 1999b

1999b *Undorosaurus* Efimov: 52.
2012 *Cryopterygius* Druckenmiller, Hurum, Knutsen & Nakrem: 313.

Type species. *Undorosaurus gorodischensis* Efimov 1999b.

Other valid species. *Undorosaurus nessovi* Efimov, 1999b; *Undorosaurus trautscholdi* Arkhangelsky & Zverkov, 2014; *Undorosaurus kielanae* (Tyborowski, 2016) comb. nov. (consideration of the latter as a valid species of *Undorosaurus* is tentative pending examination of the holotype of *Cryopterygius kielanae*).

Emended diagnosis. Moderate to large ophthalmosaurid, 3–6 m long, characterized by the following autapomorphies (marked with an asterisk) and unique character combinations: large and massive skull (almost 0.25 of total length of the animal) and robust elongated rostrum with snout ratio of 0.61; expanded postorbital region (as in *Grendelius*, *Caypullisaurus* and *Platypterygius* spp.); orbital ratio of 0.19 (0.18 in *Grendelius*); supranarial process of premaxilla strongly reduced and not contacting the external naris (well-developed supranarial process contacting the external naris in *Grendelius* and *Caypullisaurus*); subnarial process contacts the jugal (as in *Grendelius* and MJML K1885); narial process of nasal present (as in *Ophthalmosaurus* and *Acamptonectes*); lacrimal does not contact the external naris (shared with *Platypterygius australis*); orbital margin of lacrimal forms distinct angle, nearly 90°*; jugal suborbital bar thick and nearly straight; jugal posterior process anteroposteriorly wide (as in *Grendelius*, *Caypullisaurus* and *Platypterygius*); anteroposteriorly broad postorbital bar due to pronounced lateral expansion of jugal and quadratojugal (as in *Grendelius*); squamosal is present and triangular in shape as in *Ophthalmosaurus*; anteroposteriorly short and mediolaterally broad parietal, with

emerging but still poorly pronounced sagittal eminence; extremely reduced depression for the cerebral hemisphere on the parietal*; robust supratemporal process of the parietal (as in *Platypterygius australis*); basioccipital with reduced extracondylar area (as in *Ophthalmosaurus* and *Acamptonectes*, but to a lesser degree than in *Grendelius* and *Platypterygius*); teardrop-shaped outline of the exoccipital facets of the basioccipital with their pointed parts directed posteriorly (as in *Sveltonectes*, *Acamptonectes* and *Plutoniosaurus*); massive basisphenoid with extensive basipterygoid processes (width to length ratio is 1.63–1.75, significantly exceeding ratios of any other ophthalmosaurids (see Supplemental Table S2): 1.5 in *Grendelius*; 1.26–1.58 in *Ophthalmosaurus* (based on the measurements of Andrews 1910); 1.26 in *Arthropterygius*; 1.37 in *Acamptonectes*; 1.3 in *Platypterygius*; and 1.2 in *Sveltonectes* and *Sisteronia*)*; short and robust paroccipital process of the opisthotic (unlike that of *Ophthalmosaurus* and *Acamptonectes*); moderately stout stapedial shaft (like that of *Ophthalmosaurus* and unlike that of *Grendelius* and *Platypterygius*); large and robust quadrate with extensive articular condyle and reduced occipital lamella; dorsoventral ridge on the posteromedial surface of the quadrate, bordering pterygoid lamella of the supratemporal (shared with *Plutoniosaurus*, pers. obs.); large robust teeth with numerous, fine, enamel striations and stout roots, squared in cross section (as in *Grendelius*); 53 teeth present in each upper jaw as in *Grendelius* and unlike *Ophthalmosaurus* (∼48); 52 presacral vertebra as in *Aegirosaurus* (∼42 in *Ophthalmosaurus*, 47 in *Grendelius*, 42 in *Athabascasaurus*, 47–54 in *Platypterygius*); coracoids with oval outline, slightly longer anteroposteriorly than mediolaterally wide, and mediolaterally wider at posterior end than at the midpoint (similar to those of *Grendelius*); relatively reduced acromial process of the scapula*; mediolaterally compressed scapular shaft, oval in cross section (as in *Ophthalmosaurus*, *Arthropterygius* and *Acamptonectes*, and distinct from the thick and rod-like forms in *Grendelius* and *Platypterygius*); slender, rod-like clavicles*; interclavicle with expanded spatulate posterior median stem (shared with *Grendelius*); relatively small forelimb bearing 5–?6 digits (as in *Ophthalmosaurus*, *Brachypterygius*, *Aegirosaurus* and *Grendelius*); humerus commonly with three distal facets – posterodistally deflected ulnar facet, distally facing radial facet and small (or even absent in some cases) anterior accessory facet; reduced deltopectoral crest of the humerus; metacarpal 5 contacting ulnare posterodistally (i.e. 'longipinnate' condition); intermedium having extensive distal contact with distal carpal 3 and anteriorly contacting distal carpal 2 (unlike in *Ophthalmosaurus*, *Arthropterygius*, *Brachypterygius* and *Aegirosaurus*); preaxial accessory digit well developed, as long as other digits; posterior edge of the ulna commonly lacking perichondral ossification and contacting neomorphic postaxial accessory element (as in *Grendelius* and *Caypullisaurus*); phalanges rounded to polygonal in outline, not tightly packed compared to *Caypullisaurus* and *Platypterygius*, but more compactly arranged than in *Ophthalmosaurus* and *Arthropterygius*; ischiopubis expanded and unfused distally*; femur with anteroposteriorly expanded distal end, bearing two distal facets; hind limb phalanges rounded like those of *Ophthalmosaurus*.

Occurrence. European Russia, Poland, Norway (Svalbard); Upper Jurassic, middle to upper Volgian (Tithonian) (see Efimov 1999b; Druckenmiller *et al.* 2012; Arkhangelsky & Zverkov 2014; Tyborowski 2016).

Comments on the synonymy of *Undorosaurus gorodischensis* and *Cryopterygius kristiansenae*. Druckenmiller *et al.* (2012, p. 337) ended their comparisons of *Cryopterygius* with other ophthalmosaurids with the following: "Based on limb morphology, particularly its humerus and ischiopubis, *Cryopterygius* is most similar to *Undorosaurus* from approximately coeval strata (Volgian/Tithonian) of Russia (Efimov 1999b). However, given other morphological differences between the two taxa, that the skull of *Undorosaurus* is largely unknown, and in light of questions regarding the taxonomic validity of *Undorosaurus*, PMO 214.578 is referred to the new taxon *Cryopterygius* pending the availability of new data." Indeed, being poorly described up to then, *Undorosaurus* was hardly available for detailed comparison. On the other hand, the features proposed to distinguish these taxa are not reliable: "however, *Undorosaurus* bears five digits in total, while there are possibly six in *Cryopterygius*. Also, both taxa differ somewhat in the morphology of the radius and ulna, the proximal carpals and particularly in the shape of the preaxial accessory element" (Druckenmiller *et al.* 2012, p. 335). In fact, the forefins of *Undorosaurus gorodischensis* and *Cryopterygius kristiansenae* are identical in overall morphology, which was shown by Arkhangelsky & Zverkov (2014) and is supported here (Fig. 2). The anterodistal facet on the right humerus of PMO 214.578 is well pronounced and excavated (see Fig. 2L, M), making the bone indistinguishable from the other known humeri of *Undorosaurus gorodischensis*, with the exception of the left humerus of the type specimen (UPM EP-II-20(572)) which has a strongly reduced anterodistal facet as does the left humerus of PMO

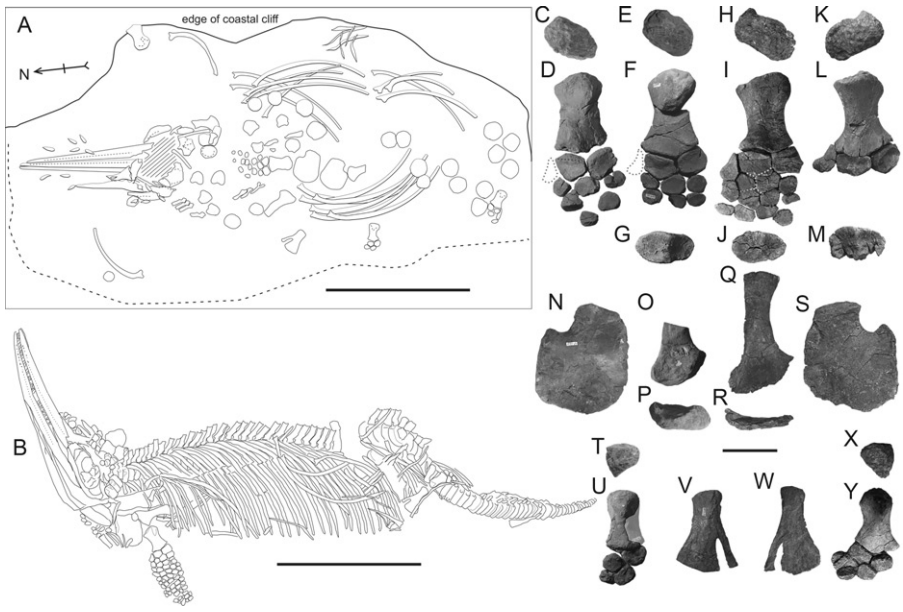

Figure 2. Comparison of type specimens of *Undorosaurus gorodischensis* and *Cryopterygius kristiansenae*. **A,** quarry map of UPM EP-II-20(572), holotype of *Undorosaurus gorodischensi*, redrawn from VME's field sketches. **B,** line drawing of the holotype of *Cryopterygius kristiansenae* (PMO 214.578), redrawn from Druckenmiller *et al*. (2012, fig. 2). **C, D,** left forelimb of UPM EP-II-20(572). **E–G,** left forelimb of UPM EP-II-21(1075). **H–J,** left forelimb of PMO 214.578. **K–M,** right forelimb of PMO 214.578; proximal end of humeri (**C, E, H, K**), dorsal views (**D, F, I**), ventral view (**L**) and distal ends of humeri (**G, J, M**). **N,** left coracoid of UPM EP-II-20(572) in dorsal view. **O, P,** proximal part of the left scapula of UPM EP-II-20(572) in lateral (**O**) and proximal (**P**) views. **Q, R,** left scapula of PMO 214.578 in lateral (**Q**) and proximal (**R**) views; note that the proximal end is strongly compressed as a result of compaction. **S,** left coracoid of PMO 214.578 in ventral view. **T, U,** right hind limb of UPM EP-II-20(572) in proximal (**T**) and ventral (**U**) view. **V,** right ischiopubis of UPM EP-II-20(572) in lateral view. **W,** left ischiopubis of PMO 214.578 in lateral view. **X, Y,** left hind limb of PMO 214.578 in proximal (**X**) and ventral (**Y**) views. Scale bars: A, B = 100 cm; C–Y = 10 cm.

214.578. Furthermore, contrary to the interpretation of Druckenmiller *et al.* (2012), the left humerus of PMO 214.578 in fact bears the anterodistal facet; it is poorly pronounced but still distinguishable (Fig. 2I, J).

Revision of the type specimens of *Undorosaurus gorodischensis* and *Cryopterygius kristiansenae* allows us to conclude that all overlapping skeletal elements (dermatocranial bones including nasal, jugal, quadratojugal; basicranial elements including basisphenoid and stapes; and postcranial elements, especially those of the appendicular skeleton) are virtually identical in both morphology (Fig. 2) and size (see Supplemental Table S1), including those diagnostic of the species *U. gorodischensis*. These are: basisphenoid with extensive anterolaterally directed basipterygoid processes; articular isometric in medial view lacking medial bulge; relatively small forelimbs; humerus with extensive and anteroposteriorly elongate proximal end, poorly pronounced trochanter dorsalis and reduced deltopectoral crest; ulna proximodistally elongate and not involved in perichondral ossification on its posterior edge; reduced pisiform facet of the ulna. Therefore, *Cryopterygius kristiansenae* Druckenmiller *et al.*, 2012 should be regarded as a junior subjective synonym of *Undorosaurus gorodischensis* Efimov, 1999b.

Undorosaurus gorodischensis Efimov, 1999b
(Figs 2–14)

v*1999b *Undorosaurus gorodischensis* Efimov: 52, figs 1a, b, 2, 3a, 4a, 5, 6.
v.1999b *Undorosaurus khorlovensis* Efimov: 57, figs 1c, d, 2c.
2000 *Undorosaurus gorodischensis* Efimov; Storrs Arkhangel'skii & Efimov: 200 [*pars*].
2000 *Ophthalmosaurus gorodischensis* (Efimov); Maisch & Matzke: 90, figs 23, 24 [*pars*].
2003 *Undorosaurus gorodischensis* Efimov; McGowan & Motani: 110, fig. 92 [*pars*].
v.2012 *Cryopterygius kristiansenae* Druckenmiller, Hurum, Knutsen & Nakrem: 313; figs 2–11.
2014 *Undorosaurus gorodischensis* Efimov; Arkhangelsky & Zverkov: 189; fig. 1C, D.
2014 *Cryopterygius kristiansenae* Druckenmiller *et al.*; Arkhangelsky & Zverkov: 189; fig. 1a.
2016 *Cryopterygius kristiansenae* Druckenmiller *et al.*; Delsett, Novis, Roberts, Koevoets, Hammer, Druckenmiller, & Hurum: figs 3a, 4b, 10a.

Holotype. UPM EP-II-20(572), incomplete disarticulated skeleton; Gorodischi, Ulyanovsk Province; Upper Jurassic, middle Volgian (Tithonian), *Epivirgatites nikitini* Ammonite Biozone.

Referred specimens. PMO 214.578 (holotype of *Cryopterygius kristiansenae*); UPM EP-II-23(744); UPM EP-II-21(1075); UPM EP-II-27(870) (holotype of *U. khorlovensis*).

Occurrence. European Russia (Moscow and Ulyanovsk provinces), Svalbard; middle to upper Volgian (Tithonian).

Diagnosis. *Undorosaurus gorodischensis* is a large (up to 6 m long) ophthalmosaurid, diagnosed relative to other species of *Undorosaurus* by the following unique character combination: extensive anterolaterally directed basipterygoid processes of the basisphenoid; teardrop-shaped stapedial head in medial view, pointed dorsally; quadrate with relatively mediolaterally compressed condyle; articular isometric in medial view, without medial bulge; relatively small forelimb (humerus to jaw length ratio *c*. 0.112; humerus length to quadrate height ratio 1.01); humerus with extensive and anteroposteriorly elongate proximal end, poorly pronounced trochanter dorsalis and deltopectoral crest; anterodistal accessory facet of the humerus is slightly pronounced; ulna posterior edge proximodistally elongate and not involved in perichondral ossification; small pisiform facet of the ulna.

Description

Skull. Taking into account that the skull of the holotype is incomplete and disarticulated, the general morphology and contacts of dermatocranial elements are based on the referred specimen PMO 214.578 (holotype of '*Cryopterygius kristiansenae*'), which had been described in great detail by Druckenmiller *et al.* (2012). Therefore, for PMO 214.578 we redescribe and discuss only some misinterpretations of Druckenmiller *et al.* (2012), and provide some additional information not previously reported.

The maxilla of PMO 214.578 was described as terminating "posteriorly at approximately the midpoint of the orbit" (Druckenmiller *et al.* 2012, p. 316), which is a misinterpretation caused by deformation of the orbital region of PMO 214.578. In fact, the maxilla only slightly contributes to the anterior portion of the suborbital bar, which is mostly formed by the jugal. The condition when the maxilla substantially contributes to the suborbital bar can be seen in, for example, *Leninia* (Fischer *et al.* 2014b).

The nasal is well preserved in the holotype UPM EP-II-20(572), allowing us to conclude that it is very similar to that of *Ophthalmosaurus* (see Andrews 1910; Moon & Kirton 2016). The *excavatio internasalis* is well pronounced on the posterodorsal part of the nasal (Fig. 3B); laterally it is surrounded by the ridge. The descending process of the nasal is present on the dorsal border of the external naris, as well as the nasal lamella, which forms a robust and short 'wing' with irregular external edge (Fig. 3A–C). Posterodorsal to the external naris there is a small embayment, which is ventrally contributed to by the dorsal border of the posterior ascending process of the maxilla in PMO 214.578 and completely enclosed within the nasal in UPM EP-II-20(572) (Fig. 3A–C). Similar foramina have been described for *Ophthalmosaurus icenicus*, *Acamptonectes densus* and *Platypterygius australis*, and may have served as passages for blood vessels and/or nerves (Kear 2005; Fischer *et al.* 2012; Moon & Kirton 2016).

The parietal, known only from the holotype UPM EP-II-20(572), is a plate-like, broad element, possessing a short and robust supratemporal process, similar to that of *Platypterygius* spp. (Kear 2005; Fischer 2012). The posterodorsal surface of the supratemporal process is rugose, forming an extensive facet for articulation with the supratemporal (Fig. 3D). The medial articular facet is subtriangular and anteroposteriorly elongated; its surface is ridged, forming a strong interdigitating suture with the contralateral parietal (Fig. 3G). The optic lobe impression is circular and extensive, whereas the portion of the impression of the cerebral hemisphere on the parietal seems to be extremely reduced compared to that of any other known ophthalmosaurid (Fig. 3E). However, it is impossible to estimate its precise size and shape due to partial crushing. The dorsal surface of the parietal is convex and smooth; medially it forms a dorsally emerging but still slightly pronounced sagittal eminence (Fig. 3F, H, I).

The squamosal is an elongate triangular and laterally compressed element that is situated at the upper part of the postorbital bar and has poor articulation with adjacent elements (Fig. 4). The right squamosal of PMO 214.578 was taphonomically displaced and is now found in the left orbit of the specimen (Supplemental Fig. S2); however, its nature was not recognized by Druckenmiller *et al.* (2012, p. 317, figs 4, 5), who described it as "another unidentified cranial element" of unclear identity, whereas the left squamosal of PMO 214.578 is still *in situ* (Fig. 4) and was not noticed by these authors.

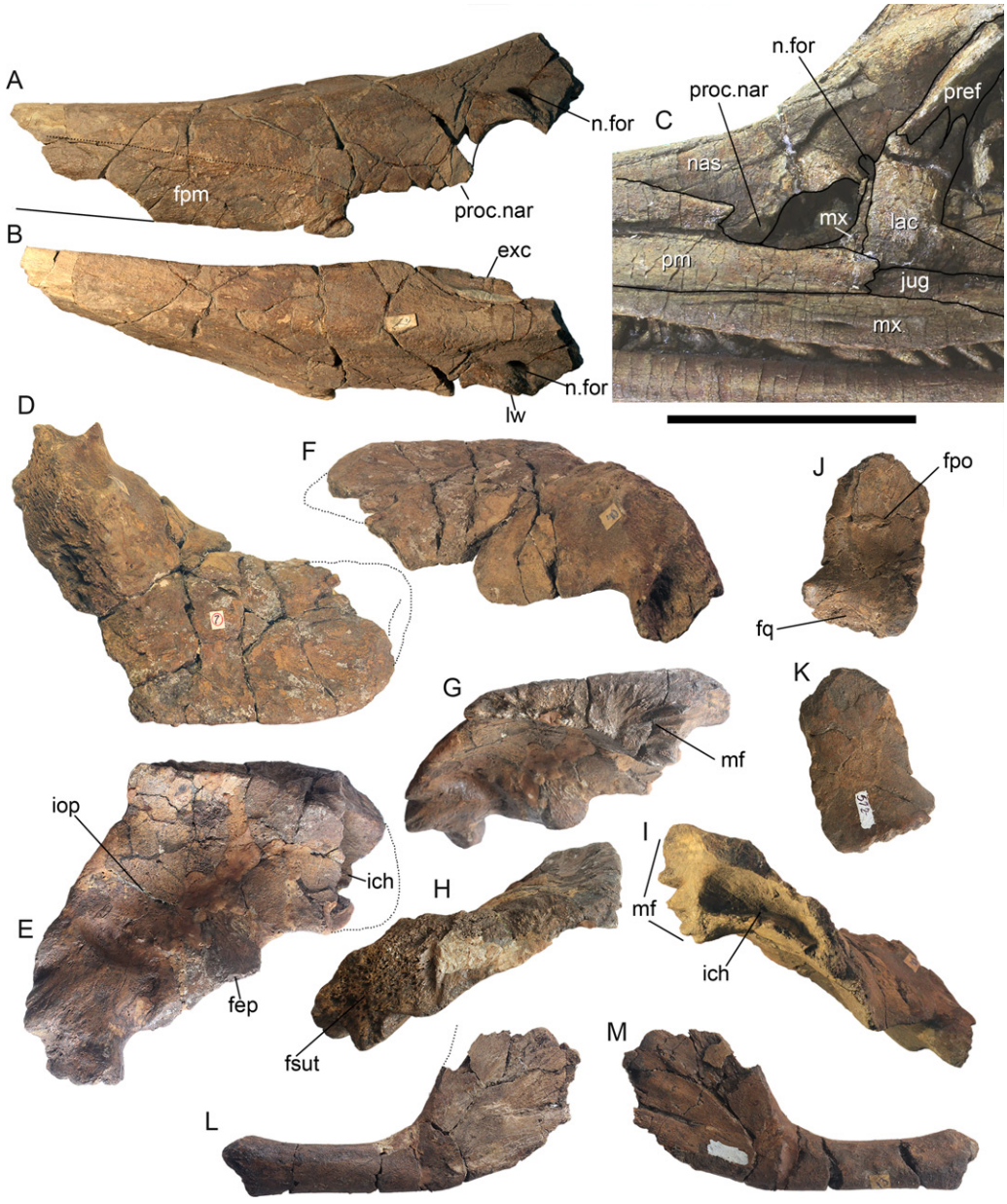

Figure 3. Cranial remains of *Undorosaurus gorodischensis.* **A, B,** left nasal of UPM EP-II-20(572), holotype, in lateral (**A**) and dorsal (**B**) views. **C,** reinterpretation of narial region of PMO 214.578. **D–I,** left parietal of UPM EP-II-20(572) in dorsal (**D**), ventral (**E**), lateral (**F**), medial (**G**), posterior (**H**) and anterior (**I**) views. **J, K,** right quadratojugal of UPM EP-II-20(572) in lateral (**J**) and medial (**K**) views; **L, M,** left jugal of UPM EP-II-20(572). Scale bar = 10 cm.

The postorbital is known only in PMO 214.578, although it is partially hidden by the displaced quadratojugal and other elements (Fig. 4). This bone appears to be relatively long anteroposteriorly; however, its dorsal contacts with other elements of the postorbital bar are not clear due to taphonomic maceration and partial displacement of this region.

The jugal is characterized by a pronounced anteroposteriorly wide posterior process, which is externally overlapped by the postorbital posterodorsally and restricted by the quadratojugal posteriorly. The posterior edge of the posterior process is irregularly digitated (Figs 3L, M, 4). The suborbital bar of the jugal is nearly straight and thickened (see Supplemental Fig. S2). The anterior flange of the jugal bears a pronounced trough along its dorsal margin and contacts the subnarial process of the premaxilla anteriorly (compare fig. 5 of Druckenmiller et al. 2012 with Fig. 3C herein).

The quadratojugal (Figs 3J, K, 4) is not reduced in length compared to that of *O. icenicus* (Moon & Kirton

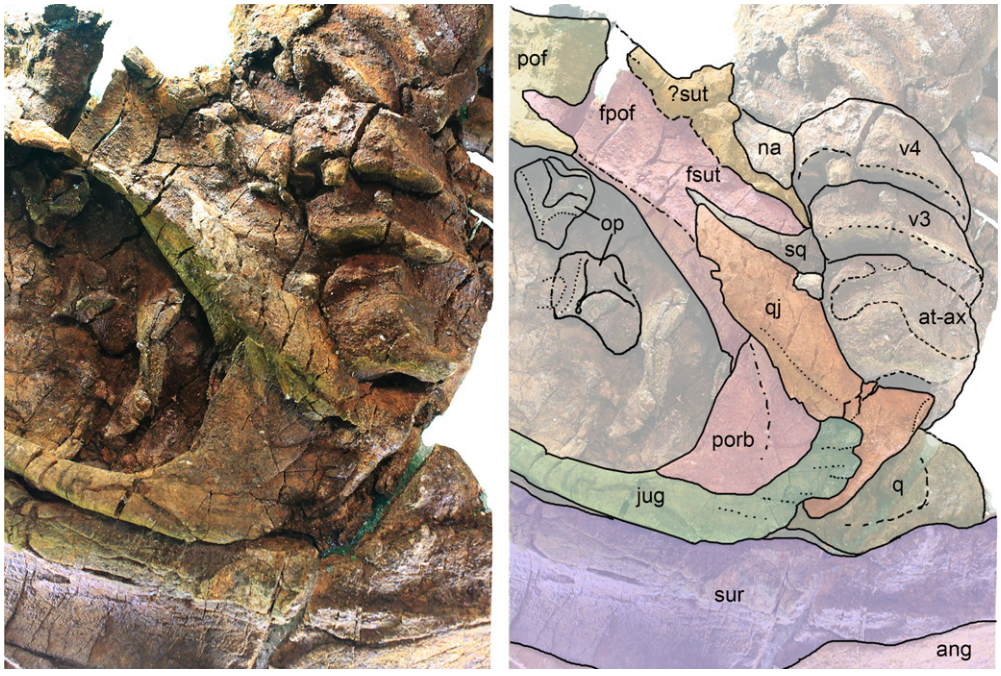

Figure 4. Postorbital region of *Undorosaurus gorodischensis*, PMO 214.578.

2016). Its posterior margin is concave and forms an acute angle with the ventral margin that bears an extensive tear-shaped facet for articulation with the quadrate (Fig. 3K). The medial surface of the quadratojugal is concave and the lateral surface bears an extensive excavated facet for articulation with other elements of the postorbital region; a similar condition was described by Fischer (2012) for *P. hercynicus*. The quadratojugal of PMO 214.578 was misinterpreted as a part of supratemporal and an element "whose identity is equivocal" (Druckenmiller *et al.* 2012, p. 316), while what was considered the quadratojugal is actually a portion of the dorsal process of the jugal (compare Fig. 6 of Druckenmiller *et al.* 2012 with Fig. 4 herein).

The quadrate is relatively large compared to those of other ophthalmosaurids. We base the description of this element on the right quadrate of the holotype (UPM EP-II-20(572)). Its anteroposterior length in the condylar region of the holotype is 120 mm and height 150 mm. In posteromedial view, the quadrate has an L-shaped outline (Fig. 5U). The occipital lamella of the quadrate is strongly reduced (Fig. 5U, W, X). The posteromedial surface of the pterygoid lamella bears a continuous dorsoventral ridge outlining the pterygoid lamella of the supratemporal (Fig. 5U). The articular condyle is divided onto two bosses: a ventrally bulging massive medial boss for the articular, and a reduced lateral boss for the surangular (Fig. 5V, W). The ventral edge of the medial boss is somewhat V-shaped (Fig. 5U). Above the condyle, the lateral edge of the quadrate bears a circular depression, the facet for the quadratojugal. The stapedial facet is a pronounced circular depression in the middle of the medial surface. The posterolateral edge of the quadrate is restricted by a shallow quadrate foramen.

Despite the poor preservation of the element in the holotype, the basioccipital could be observed from two referred specimens (UPM EP-II-21(1075) [Fig. 6 A–D] and PMO 214.578) and one specimen from the type series UPM EP-II-22(1073) here referred to as *Undorosaurus* sp. The basioccipital is a massive element, possessing a spherical condyle and reduced extracondylar area (Fig. 4A–G). Despite being reduced, the extracondylar area is still visible in posterior and ventral views to a similar degree to that of *Ophthalmosaurus icenicus* and *Acamptonectes densus*. The ventral notch is not pronounced in UPM EP-II-21(1075) (Fig. 6D). The notochordal pit is pronounced as a vertical depression formed by two deep pits situated in the dorsal half of the condyle (Fig. 6A, E). The exoccipital facets are teardrop shaped in outline, and their pointed parts are directed posteriorly (Fig. 6C, G). The base of the foramen magnum is also teardrop shaped, restricted by the medial margins of the two exoccipital facets, which are nearly confluent but still separate anteriorly. The posterior embayment of the foramen magnum is wide (Fig. 6C, G). In lateral view the basioccipital is relatively long, possessing an anteroposteriorly elongated extracondylar area, similar to that of *Arthropterygius chrisorum* and *Palvennia hoybergeti* (Maxwell 2010;

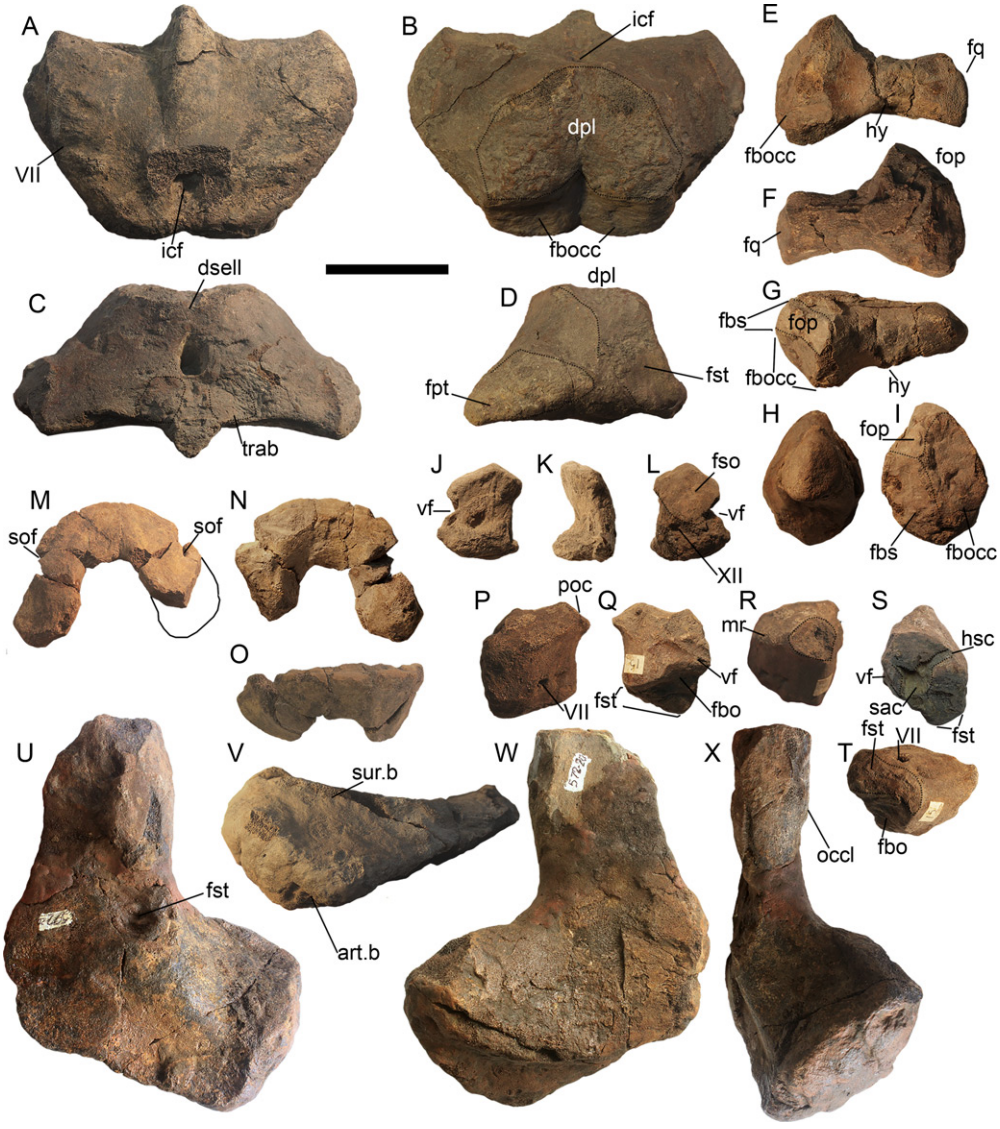

Figure 5. Basicranial region elements and quadrate of *Undorosaurus gorodischensis*, UPM EP-II-20(572), holotype. **A–D,** basisphenoid in ventral (**A**), dorsal (**B**), anterior (**C**) and lateral (**D**) views. **E–I,** right stapes in posterior (**E**), anterior (**F**), dorsal (**G**), lateral (**H**) and medial (**I**) views. **J–L,** right exoccipital in medial (**J**), posterior (**K**) and lateral (**L**) views. **M–O,** supraoccipital in posterior (**M**), anterior (**N**) and dorsal (**O**) views. **P–T,** left opisthotic in anterior (**P**), posterior (**Q**), lateral (**R**), medial (**S**) and ventral (**T**) views. **U–X,** right quadrate in posteromedial (**U**), ventral (**V**), anterolateral (**W**) and posterolateral (**X**) views. Scale bar = 5 cm.

Druckenmiller *et al.* 2012) and unlike the condition in *Grendelius* spp. (McGowan 1976; Zverkov *et al.* 2015a). The stapedial and opisthotic facets of the basioccipital are well pronounced in lateral view; they are nearly equal in size and similar in outline to each other (Fig. 6B).

The basisphenoid is a massive element with extensive anterolaterally directed basipterygoid processes (Fig. 5A, B). It is somewhat trapezoidal in ventral outline, resembling that of *Grendelius* (McGowan 1976; Zverkov *et al.* 2015a). The ratio of mediolateral maximum width to anteroposterior length is 1.63. The posterior foramen for the internal carotid arteries is situated in the posterior half of the basisphenoid ventral surface, closer to its posterior margin (Fig. 5A). The anterior surface of the basisphenoid is high and wide (Fig. 5C). The basisphenoid is trapezoidal in lateral view, being dorsally bounded by a well-pronounced dorsal plateau. The basioccipital facet of the basisphenoid faces posteriorly, as in most ophthalmosaurids and unlike in *Arthropterygius* (Maxwell 2010; Zverkov *et al.* 2015b).

The supraoccipital is an arched C-shaped element (Fig. 5M, N). It is known only from UPM EP-II-20(572). Its ventral extension is reduced, making this part of the bone less massive than that of many other ophthalmosaurids (see Andrews 1910; Kuhn 1946; Kear

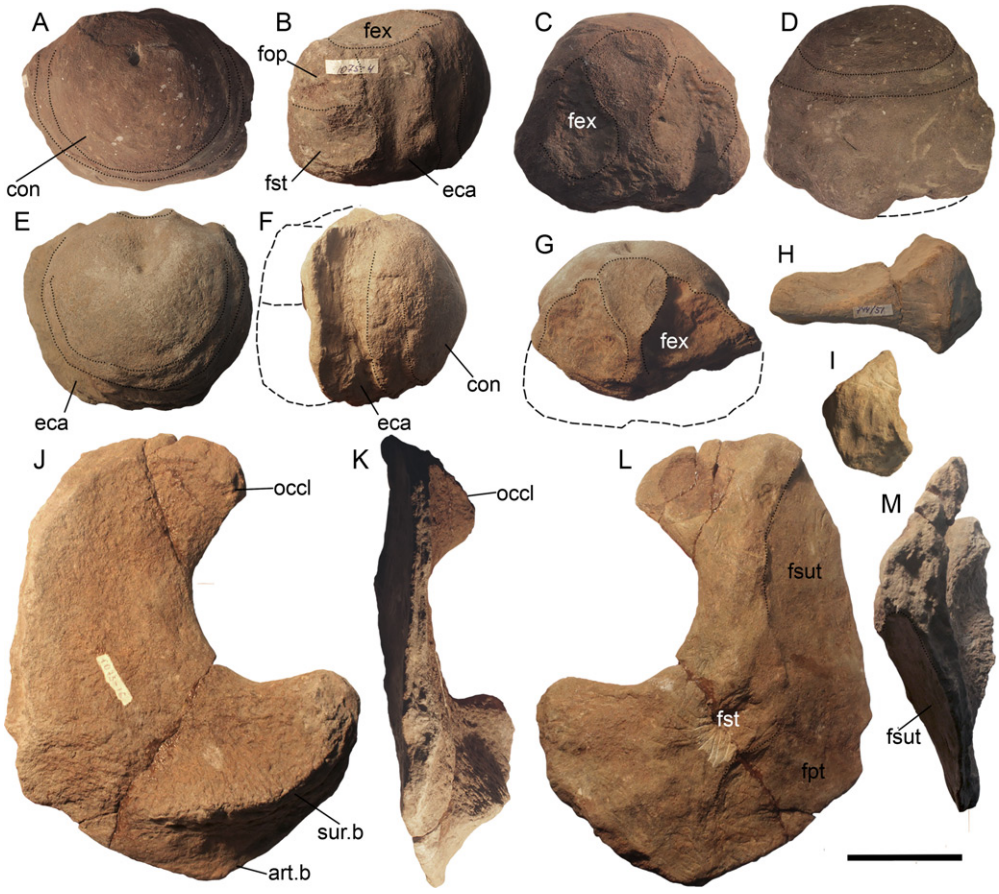

Figure 6. Basioccipitals, stapes and quadrate of *Undorosaurus*. **A–D,** basioccipital of *Undorosaurus gorodischensis*, UPM EP-II-21(1075), in posterior (**A**), left lateral (**B**), dorsal (**C**) and ventral (**D**) views. **E–G,** basioccipital of *Undorosaurus* sp., UPM EP-II-22(1073), in posterior (**E**), left lateral (**F**) and dorsal (**G**) views. **H, I,** left stapes of *Undorosaurus gorodischensis*, UPM EP-II-23(744), in posterior (**H**) and medial (**I**) views. **J–M,** left quadrate of *Undorosaurus* sp., UPM EP-II-22(1073), in anterolateral (**J**), anteromedial (**K**), posteromedial (**L**) and dorsal (**M**) views. Scale bar = 5 cm.

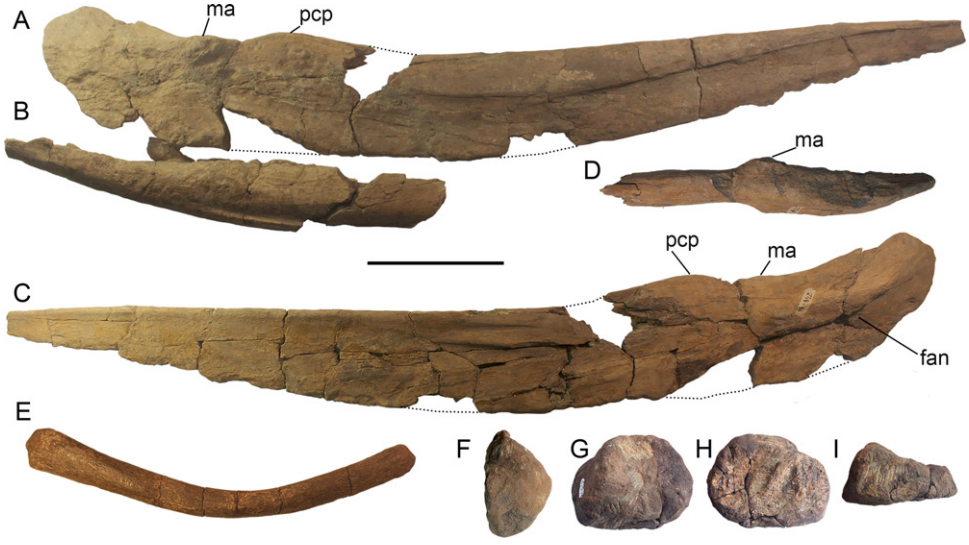

Figure 7. Mandibular and hyolaryngeal elements of *Undorosaurus gorodischensis.* **A, C, D,** left surangular of UPM EP-II-23(744) in medial (**A**), lateral (**C**) and dorsal (**D**) views. **B,** partial left angular of UPM EP-II-23(744) in medial view. **E,** cornu branchiale I of UPM EP-II-22(1073). **F–I,** right articular of UPM EP-II-20(572), holotype, in anterior (**F**), medial (**G**), lateral (**H**) and ventral (**I**) views. Scale bar = 10 cm.

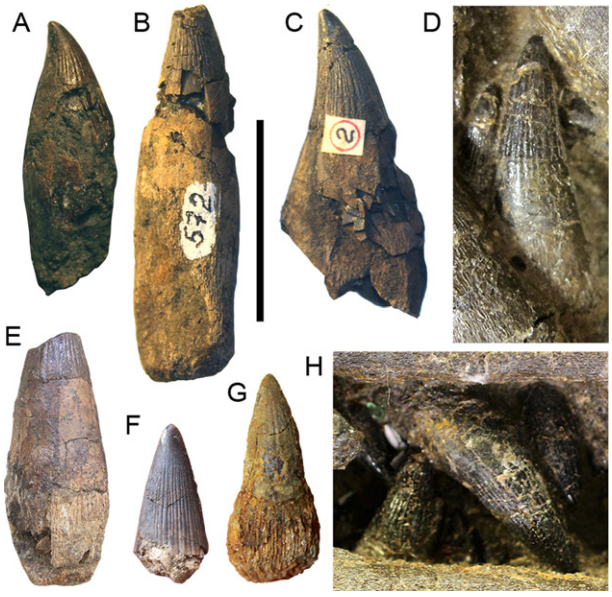

Figure 8. Teeth of *Undorosaurus gorodischensis.* **A–C,** UPM EP-II-20(572), holotype; **D, G, H,** PMO 214.578; **E, F,** UPM EP-II-23(744). Scale bar = 3 cm.

2005; Druckenmiller *et al.* 2012; Fischer *et al.* 2014a; Moon & Kirton 2016). The lateral otic impressions are poorly visible, probably due to bad preservation. A foramen endolymphaticum (*sensu* McGowan 1973; Maisch 2002; Maisch & Matzke 2006) or a foramen for a vein (as interpreted by Moon & Kirton 2016) is well pronounced, with a groove to the dorsolateral border of the supraoccipital (Fig. 5M).

The exoccipital is known only for UPM EP-II-20(572) (Fig. 5J–L). It is a columnar element with an anteroposteriorly short occipital foot, resulting in two hypoglossal foramina on the medial side, and only one on the lateral side. The base of the occipital foot is anteriorly rounded and slightly pointed posteriorly.

The opisthotic has a robust and shortened paroccipital process (Fig. 5P, Q). It is better preserved in UPM EP-II-20(572) on which we base the following description. The lateral muscular ridge (for attachment of the *M. adductor mandibulae externus*) is well pronounced (Fig. 5P, R). The medioventral surface of the opisthotic is divided into a large, rugose, posteroventrally facing facet for the basioccipital and a smaller, elongated facet

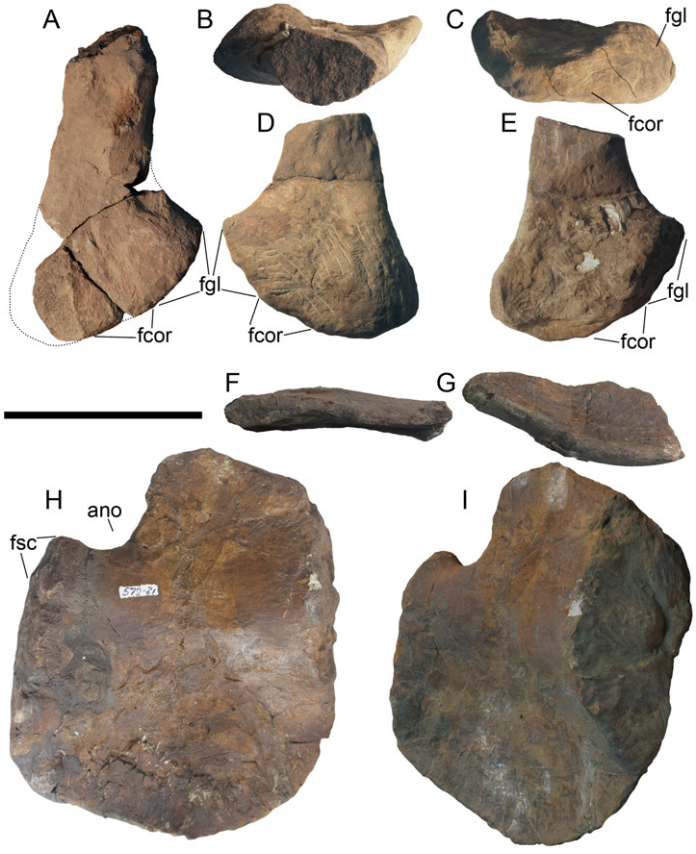

Figure 9. Pectoral girdle elements of *Undorosaurus gorodischensis*, UPM EP-II-20(572), holotype. **A,** right scapula in lateral view. **B–E,** left scapula in proximal (**C**), medial (**D**) and lateral (**E**) views; cross section of the shaft (**B**). **F, G,** fragmental clavicle. **H, I,** left coracoid in dorsal (**H**) and oblique medial (**I**) views. Scale bar = 10 cm.

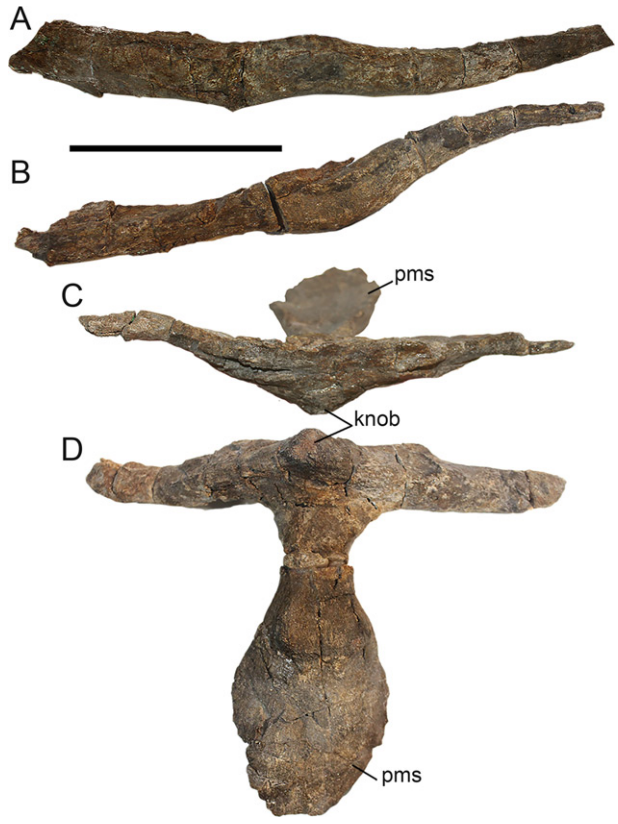

Figure 10. Pectoral girdle elements of *Undorosaurus gorodischensis*, PMO 214.578. **A, B,** left clavicle in anterior (**A**) and ventral (**B**) views. **C, D,** interclavicle in anterior (**C**) and ventral (**D**) views. Scale bar = 10 cm.

for the stapes (Fig. 5Q, T). The stapedial facet of UPM EP-II-20(572) is not divided by a groove that probably housed the VII or the IX nerve (as occurs in all other ophthalmosaurids; e.g. Moon & Kirton 2016). The canal of this nerve is immersed in the body of the bone and opens on its posteroventral surface by a marked foramen (Fig. 5Q, T). This could be autapomorphic for *Undorosaurus*; however, variations are possible and pending data from the other specimens we avoid considering this feature autapomorphic. The otic capsule is deeply impressed in the opisthotic (Figs 4, 5S). The impression of the sacculus is relatively small; the impression for the horizontal semicircular canal is deep and elongate (Figs 4, 5S).

The stapes is well preserved in UPM EP-II-20(572) (Fig. 5E–I) and also known from UPM EP-II-23(744) (Fig. 6H, I). It is similar to that of *Ophthalmosaurus* (see Moon & Kirton 2016): the stapedial shaft is moderately stout and the medial head of the stapes is oval in outline with slightly tapering dorsal part, which bears the opisthotic facet. The facet for the opisthotic is triangular in outline and poorly pronounced (reduced in comparison to other ophthalmosaurids). Facets for the basioccipital and basisphenoid are semicircular and equal in size (Fig. 5I). The hyoid process is poorly pronounced but still visible on the posterior surface of the element (Fig. 5E, G).

A hyoid element preserved in UPM EP-22(1073) is a curved 28 cm long rod that is subcircular in cross section for most of its length and slightly expanded at both ends (Fig. 7E).

Mandible. As the morphology of the mandibular bones was described for PMO 214.578 by Druckenmiller *et al.* (2012), we concentrate on additional data available from isolated bones in the UPM material. The surangular in PMO 214.578 is largely obscured by the angular, prearticular and articular, so that only its posterodistal portion is exposed; therefore, the isolated and nearly complete left surangular of UPM EP-II-23(744) reveals additional anatomical information. The surangular is an elongate plate-like element, thickened along its dorsal margin; it is practically indistinguishable from that of *Ophthalmosaurus icenicus* (see Moon & Kirton 2016). The posterior portion of the surangular is dorsoventrally expanded and has a rounded posterior margin. The medial surface of the surangular bears a concavity comprising the lateral wall of the Meckelian canal. The fossa surangularis, which probably housed nerves and blood vessels, runs along the lateral surface of the surangular and continues posteriorly to a foramen that pierces the bone and opens medially; this foramen is relatively small in UPM EP-II-23(744). The paracoronoid process is low and rounded; posterior to it, the lateral margin of the surangular forms a small ridge, which probably functioned as attachment point of the *Musculus adductor mandibulae externus* (according to Moon & Kirton 2016; Fig. 7A, C).

The angular present in some specimens of the type series (e.g. UPM EP-II-22(1073); Fig. 7B) is too poorly preserved for a detailed description.

The articular is a compact element, isometric in outline, which forms the posterior surface of the glenoid articulation with the quadrate condyle. Its anterior part is strongly thickened and forms a teardrop-shaped anterior surface (Fig. 7F), which is inclined posterodorsally; this surface is pitted and likely was continued anteriorly by the articular cartilage. The medial face of the element is saddle shaped for the articulation with the quadrate; the lateral face is slightly convex and rugose to meet the surangular laterally (Fig. 7H). The posterior edge of the articular is rounded; it lacks perichondral ossification, which indicates posterior cartilage continuation.

Dentition. The teeth are robust, having long roots that are semicircular to square in cross section, and conical crowns (Fig. 8). The largest tooth is 65 mm high apicobasally and 15 mm in maximum diameter across

Figure 11. Forelimb elements of *Undorosaurus gorodischensis.* **A,** incomplete left forelimb of UPM EP-II-20(572), holotype, in dorsal view; **B,** humeral proximal end of the same specimen. **C–E,** incomplete left forelimb of UPM EP-II-23(744); **C,** humeral proximal end; **D,** dorsal view; **E,** humeral distal end. **F,** incomplete left forelimb, YKM 44028-7, in ventral view. **G–K,** incomplete left forelimb of UPM EP-II-21(1075); **G,** dorsal view; humerus in ventral (**H**), anterior (**I**), distal (**J**) and proximal (**K**) views. Scale bar = 10 cm.

the root. The crowns are slightly curved and ornamented with tightly packed apicobasal enamel ridges, which terminate before reaching the apex. The apicobasal length of the largest crown is 21 mm. The base of the enamel layer in some teeth is poorly defined, but still distinguishable. The region between the crown and root appears smooth; only in some teeth does it bear additional plicidentine folding immediately basal to the crown (Fig. 8D).

Axial skeleton. It is impossible to estimate the total number of vertebrae in any of the specimens from the type series; however, isolated centra were described and figured by Efimov (1999b). A continuous and nearly articulated preflexural series is known for PMO 214.578 (Druckenmiller *et al.* 2012). For details on the morphology of the *Undorosaurus gorodischensis* axial skeleton, see Efimov (1999b) and Druckenmiller *et al.* (2012).

Pectoral girdle and forelimb. The scapula is characterized by a curved, strap-like shaft that gradually becomes flared and thickened proximally, forming a proximal blade (Fig. 9A–E). The proximal blade of the element is a slightly S-shaped curve; it forms a relatively small acromial process anteriorly and a facet for the coracoid as well as a slightly broadened glenoid contribution posteriorly. The glenoid contribution is equal in size to the coracoid facet (Fig. 9C).

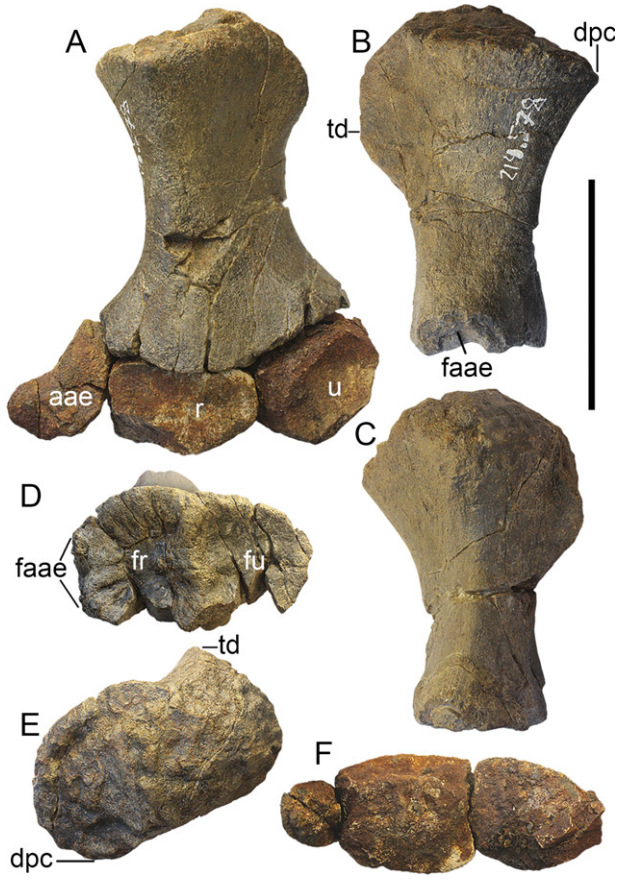

Figure 12. Right forelimb of *Undorosaurus gorodischensis*, PMO 214.578. **A,** humerus and associated epipodial elements in ventral view. **B–E,** humerus in anterior (**B**), posterior (**C**), distal (**D**) and proximal (**E**) views. **F,** proximal articular surfaces of the epipodial elements. Scale bar = 10 cm.

The coracoid (Fig. 9H, I) is a plate-like element, oval in outline, which is anteroposteriorly longer than mediolaterally wide (the length-to-width ratio is 1.2 in the holotype and PMO 214.578). The medial articular facet of the coracoid is thickened and somewhat lenticular in outline; it forms the anterior half of the medial margin (Fig. 9I). The lateral scapular facet is markedly smaller than the glenoid contribution. The angle between the surface of the glenoid contribution and the medial surface is obtuse, so the facets are poorly demarcated (Fig. 9H). The anteromedial process, divided from the lateral surface by a prominent anterior notch, is wide and sheet-like as in most other Jurassic ophthalmosaurids. The posterior end is the widest part of the element; it is strongly compressed dorsoventrally.

The clavicle is better preserved in PMO 214.578. It is a slender and rod-like paired element. Its medial end is relatively low and thick compared to that of other ophthalmosaurids (Figs 9F, G, 10A, B), which could be regarded as an autapomorphy of *Undorosaurus*. The lateral ramus of the clavicle is rod-like, curved dorsomedially where it contacts the scapular shaft (Fig. 10A).

The interclavicle, known only for PMO 214.578, is a large triradiate element with slender lateral rami and an extensive spatulate posterior median stem (Fig. 10D). The ventral and anterior surfaces are divided by a ridge that forms a pointed knob in its middle (Fig. 10C, D), similar to that of *Grendelius alekseevi* (see Zverkov *et al.* 2015a).

The humerus bears three distal facets: a posterodistally deflected ulnar facet and distally facing radial facet, which are nearly equal in anteroposterior length, and a small (or even nearly absent in some specimens; see discussion) anterior facet for the accessory epipodial element (Figs 11–13). The proximal and distal ends of the humerus are nearly equal in anteroposterior width, with the proximal end only slightly broader. The proximal articular surface is anteroposteriorly longer than dorsoventrally tall (Figs 11B, C, K, 12E, 13E, J). The dorsal trochanter is a pronounced, oblique ridge; the deltopectoral crest is poorly pronounced, as in *Ophthalmosaurus* and *Arthropterygius*.

There are three epipodial elements: ulna, radius and a preaxial accessory element. The ulna is a roughly hexagonal element with three distal facets for the intermedium, ulnare and pisiform. The posterior edge of the ulna lacks perichondral ossification and probably *in vivo* contacted a postaxial accessory neomorphic element (as in other species of the genus); however, none of the specimens referred to as *Undorosaurus gorodischensis* has this element preserved.

The radius is symmetrically pentagonal with the proximal articular surface being the widest and slightly convex (Figs 11A, D, F, G, 12A). Distally it bears two distinct facets for the intermedium and radiale; the anterior facet for the accessory element commonly faces directly anteriorly and is demarcated from the facet for the radiale; however, in the left limb of the holotype (UPM EP-II-20(572)) these facets are poorly demarcated (Fig. 11A).

The autopodial elements are oval to polygonal with rounded corners (Fig. 11F); they are not so tightly packed as in more derived ophthalmosaurids (e.g. *Platypterygius* spp., *Sveltonectes insolitus*, *Maiaspondylus lindoei*), but not as loose as in *Ophthalmosaurus* (Moon & Kirton 2016). The ulnare bears a distal facet for distal carpal 4 and a smaller posterodistal facet for metacarpal 5; this is the 'longipinnate' condition *sensu* Zverkov *et al.* (2015a).

The intermedium is proximodistally short and anteroposteriorly elongate with an extensive distal facet for distal carpal 3, and a small anterodistal facet for distal

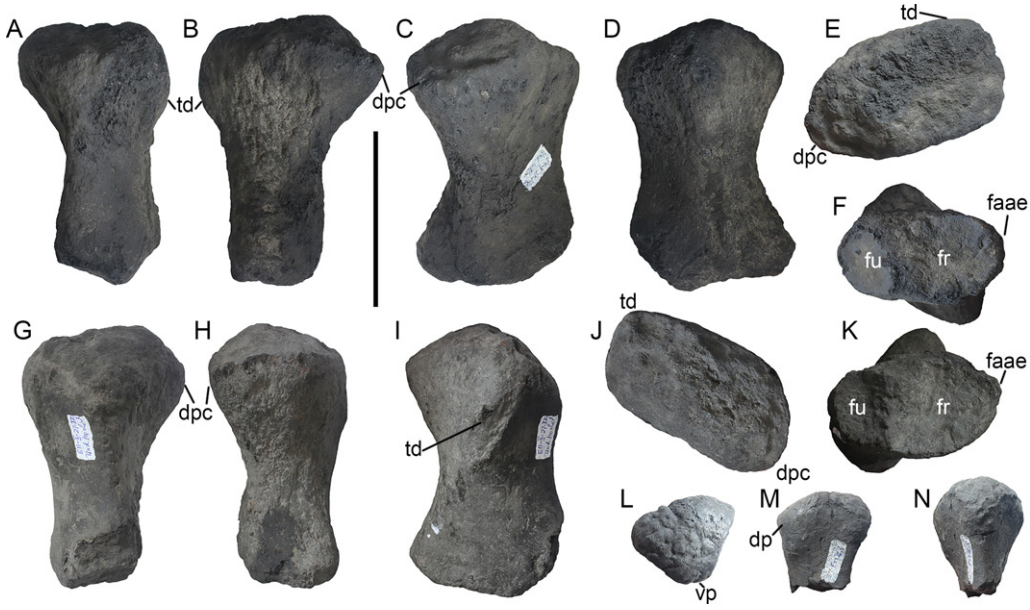

Figure 13. Humeri and partial femur of UPM EP-II-27(870), holotype of *Undorosaurus khorlovensis*, here synonymized with *Undorosaurus gorodischensis*. **A–F,** right humerus; **G–K,** left humerus; **L–N,** proximal portion of left femur. **A, G, N,** posterior views; **B, H,** anterior views; **C,** ventral view; **D, I, M,** dorsal views; **E, J, L,** views of proximal end; **F, K,** views of distal end. Scale bar = 10 cm.

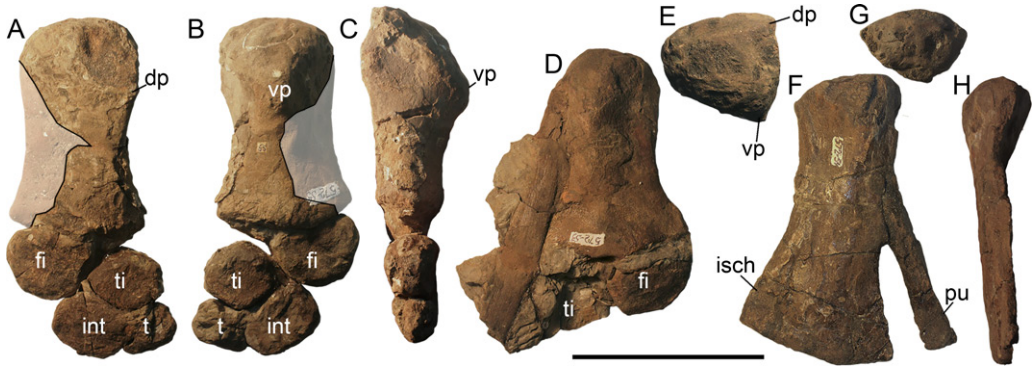

Figure 14. Pelvic girdle and hind limbs of *Undorosaurus gorodischensis*, UPM EP-II-20(572), holotype. **A–C,** partial right hind limb in dorsal (**A**), ventral (**B**) and anterior (**C**) views. **D, E,** left femur with associated epipodial elements in dorsal view (**D**), and its proximal end (**E**). **F–H,** right ischiopubis in ventral (**F**), proximal (**G**) and anterior (**H**) views. Scale bar = 10 cm.

carpal 2. The preaxial accessory digit is well developed and as long as the other digits.

Pelvic girdle and hind limb. The ischiopubis is a complex, mediolaterally compressed element, thickened only in its acetabular (proximal) portion. This element is known from the holotype (Fig. 2V) and PMO 214.578 (Fig. 2W). The most peculiar feature of the element is that the ischium and pubis, being fused along half of their length, are split medially. This is not the ancestral state for Neoichthyosauria; considering its morphology, distinct from that of basal Thunnosauria, it is likely a derived condition. The ischium is markedly broader than the pubis, forming most of the element (Fig. 14F).

Both hind limbs are preserved but they are partially disarticulated in the holotype. The femur is similar to that of *Ophthalmosaurus* (see Moon & Kirton 2016). The distal end of the bone is slightly wider than the proximal end. The femur-to-humerus length ratio is 0.69 in the holotype (0.72 in PMO 214.578). The posterior margin of the femur is tapered, whereas the anterior surface is convex. Both the ventral and dorsal processes are slightly pronounced (Fig. 14C, E). The ventral process is shifted anteriorly; similarly, the dorsal process originates near the anterior margin of the femur. There are two distal facets of nearly equal length.

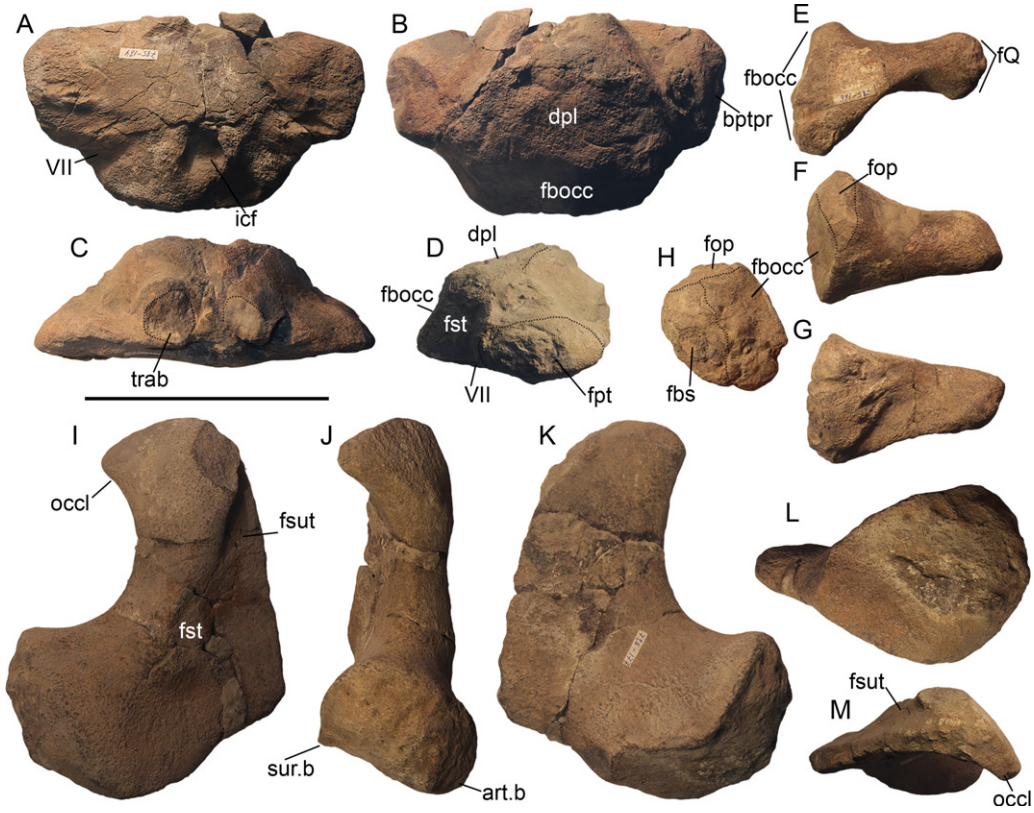

Figure 15. Basicranial region elements and quadrate of *Undorosaurus nessovi*, UPM EP-II-24(785), holotype. **A–D,** basisphenoid in ventral (**A**), dorsal (**B**), anterior (**C**) and lateral (**D**) views. **E–H,** right stapes in posterior (**E**), dorsal (**F**), ventral (**G**) and medial (**H**) views. **I–M,** left quadrate in posteromedial (**I**), lateral (**J**), anterolateral (**K**), ventral (**L**) and dorsal (**M**) views. Scale bar = 10 cm.

The tibia is a small element, pentagonal in dorsal view, with an anterior facet for the preaxial accessory element, whereas there is no facet for the anterior accessory element on the femur in the holotype (the preaxial accessory element was probably in contact with the femur in PMO 214.578). The fibula is bigger than the tibia; it is irregularly hexagonal with a posterodistal facet for a postaxial ossicle, a distal facet for the fibulare (calcaneum), an anterodistal facet for the intermedium (astragalus; depending on interpretive paradigm), and an anterior facet for the tibia.

Undorosaurus nessovi Efimov, 1999b
(Figs 15–17)

v*1999b *Undorosaurus nessovi* Efimov: 56; figs 1f, 3b, 4b.
2000 *Undorosaurus gorodischensis* Efimov; Storrs, Arkhangel'skii & Efimov: 200 [*pars*].
2000 *Ophthalmosaurus gorodischensis* (Efimov); Maisch & Matzke: 90; fig. 28 [*pars*].
2003 *Undorosaurus gorodischensis* Efimov; McGowan & Motani: 110 [*pars*].
2012 *Undorosaurus* '*nessovi*' c.f. *gorodischensis* Efimov; Druckenmiller, Hurum, Knutsen & Nakrem: 336; fig. 22G.
2014 *Undorosaurus gorodischensis* Efimov; Arkhangelsky & Zverkov: 189; fig. 1B [*pars*].

Holotype and only known specimen. UPM EP-II-24(785), a disarticulated skeleton, including incomplete right mandibular ramus, basisphenoid, basioccipital (heavily eroded), right stapes, both quadrates, articular and surangular, hyoid, atlas-axis and 15 vertebrae, rib fragments, coracoid, scapulae, and nearly complete right and fragmental left forelimbs.

Occurrence. Type locality only; bank of the Volga River near Slantsevy Rudnik village, Ulyanovsk Province; Upper Jurassic, middle Volgian (Tithonian), *Virgatites virgatus* Ammonite Biozone.

Diagnosis. *Undorosaurus nessovi* can be diagnosed relative to other species of *Undorosaurus* by the following unique character combination: posterolaterally directed basipterygoid processes of the basisphenoid; circular stapedial head in medial view; completely reduced hyoid process of the stapes and raised stapedial shaft; moderate-sized quadrate with robust and reduced occipital lamella and massive mediolaterally broadened condyle; articular rhomboidal in medial view with protruding

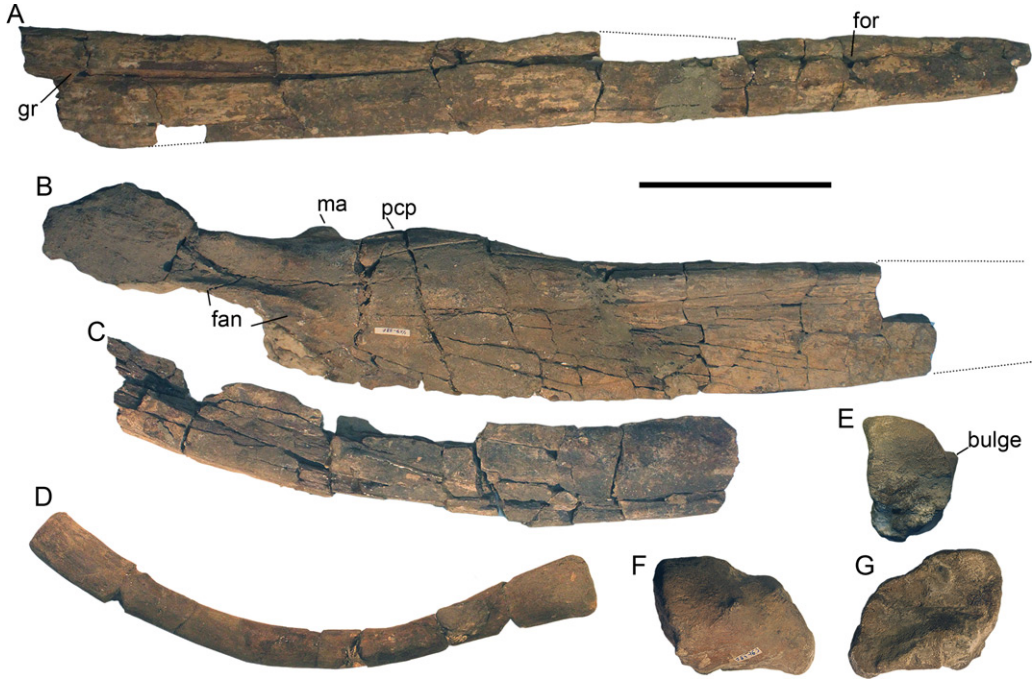

Figure 16. Mandibular and hyolaryngeal elements of *Undorosaurus nessovi*, UPM EP-II-24(785), holotype. **A,** right dentary in lateral view. **B,** right surangular in lateral view. **C,** partial right angular in lateral view. **D,** cornu branchiale I. **E–G**, right articular in anterior (**E**), medial (**F**) and lateral (**G**) views. Scale bar = 10 cm.

posterior end and pronounced bulge on the medial articular surface*; relatively large forelimbs (humerus-to-jaw length ratio *c.* 0.183; humerus length-to-quadrate height ratio 1.22); slender humerus with distal end wider than proximal; isometric, subcircular proximal end of the humerus; proximodistally shortened ulna with posterior edge not involved in perichondral ossification and bearing two pronounced facets for the pisiform and the neomorph.

Description.

Skull. The quadrate is a massive and robust element 155 mm dorsoventrally high and 118 mm anteroposteriorly long in the condylar region. In posteromedial view, the quadrate has an L-shaped outline (Fig. 15I), which is common for derived Cretaceous ophthalmosaurids (e.g. Fischer *et al.* 2014a). The posterolateral edge of the quadrate is restricted by the shallow quadrate foramen (Fig. 15I, K). The condyle is massive, bulbous and strongly convex in medial view; its articular surface bears a shallow concavity, which only slightly divides the articular and surangular bosses (Fig. 15L). The posteromedial surface of the quadrate bears a continuous dorsoventral ridge bordering the pterygoid lamella of the supratemporal (Fig. 15I). Judging the shape of the facet for the supratemporal, which is nearly confluent with the stapedial facet, it is likely that the stapes was in contact with the supratemporal. The stapedial facet is a well-pronounced circular depression in the middle of the medial surface.

The basioccipital is severely weathered; therefore, an accurate description cannot be provided.

The basisphenoid has extensive and slightly posterolaterally directed basipterygoid processes (Fig. 15A). It is anteroposteriorly shorter than mediolaterally wide, having an unprecedentedly high width-to-length ratio among ophthalmosaurids (1.75). The posterior foramen for the internal carotid arteries is situated in the posterior half of the basisphenoid ventral surface, being closer to the middle than that of the type species (Fig. 15A). In lateral view, the basisphenoid is roughly trapezoid. The dorsal plateau is expansive and pentagonal in outline. The basioccipital facet of the basisphenoid is rectangular in outline and faces posteriorly.

The stapes is similar to that of the type species: the stapedial shaft is moderately stout and the medial head of the stapes is oval in outline (Fig. 15H). The stapedial shaft is slightly raised relative to the condyle. The facet for the opisthotic is triangular in outline, slightly shifted anteriorly and poorly pronounced. Facets for the basioccipital and basisphenoid are nearly equal in size. The hyoid process is poorly pronounced as a shallow ridge that obliquely continues from the ventral medial

Figure 17. Forelimb and pectoral girdle elements of *Undorosaurus nessovi*, UPM EP-II-24(785), holotype. **A,** right forelimb in dorsal view. **B–F,** humerus in anterior (**B**), ventral (**C**), posterior (**D**), distal (**E**) and proximal (**F**) views. **G–I,** ulnae in posterior (**G, I**) and dorsal (**H**) views. **J,** fragmental coracoid. **K–P**, scapulae in external (**N, K**), posterior (**L**) and proximal (**O, P**) views. **Q**, proximal articular surfaces of the epipodial elements. Scale bar = 10 cm.

corner of the stapedial head to the middle of the shaft (Fig. 15E).

A hyoid element is a curved 30 cm long rod that is expanded at both ends and subcircular in cross section for most of its length (Fig. 16D).

Mandible. The right mandibular ramus is preserved, represented by the anterior portion of the dentary, the posterior part of the surangular and a fragment of the angular. All the elements are similar to those of the type species. The estimated total length of the mandible is *c*. 100 cm. The dentary bears a deep lateral groove that becomes discontinuous anteriorly, being largely contained as a canal within the bone, and opening via foramina. These foramina continue anteriorly as a complex of grooves, which ornament the lateral surface of the dentary at the tip of the snout (Fig. 16A). The surangular is characterized by a well-pronounced ridge of the *M. adductor mandibulae externus*, which is directed mediodorsally and visible even in lateral view (Fig. 16B).

The articular is rhomboid in medial view. Its anterior part is strongly thickened forming a surface that is teardrop shaped in outline, which is slightly excavated (Fig. 16E); this surface is inclined ventrally. The medial face of the articular is saddle shaped for the articulation with the quadrate. In its middle there is a pronounced medial bulge (Fig. 16E, F), which is an autapomorphy of *U. nessovi* (a similar bulge is also present in *Sveltonectes insolitus* (Fischer *et al*. 2011), *Platypterygius australis* (Kear 2005) and '*Yasykovia yasykovi*' Efimov, 1999a,

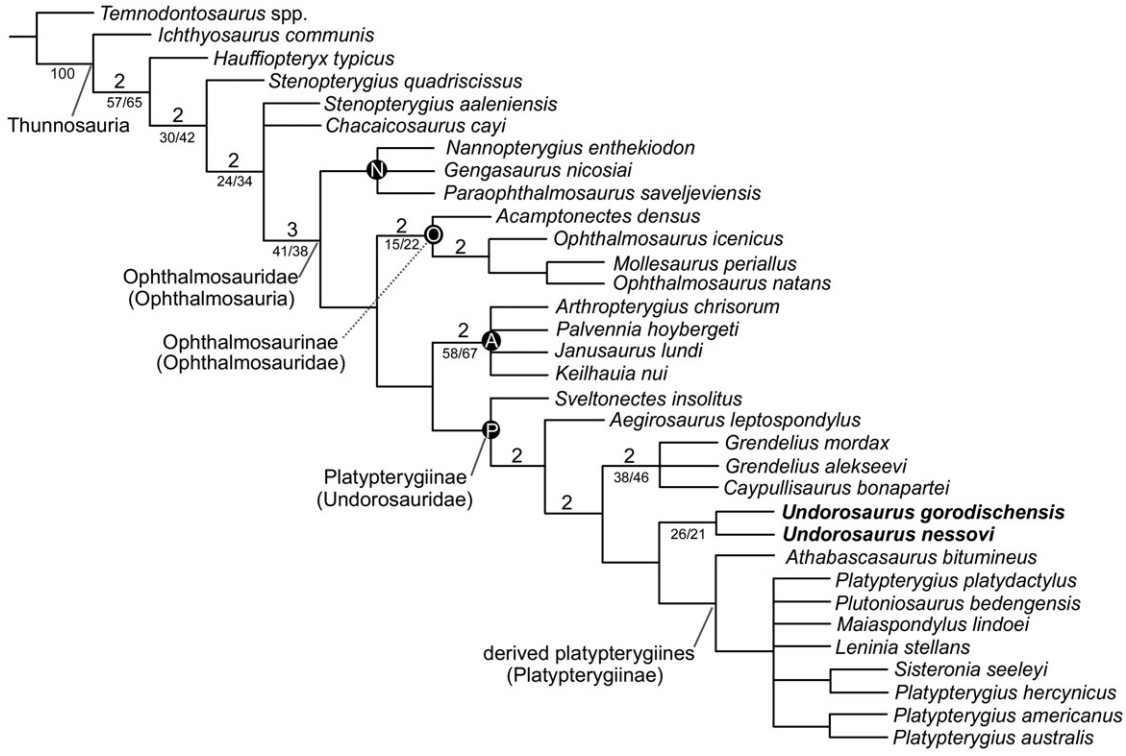

Figure 18. Phylogeny of Thunnosauria based on strict consensus tree. Bremer support values >1 are shown above the branches; bootstrap/jackknife support values of greater than 20 are indicated below the branches. Abbreviations: A, *Arthropterygius* clade; N, *Nannopterygius* clade; O, Ophthalmosaurinae; P, Platypterygiinae. Another possible taxonomic context for the recovered phylogeny is given in parentheses.

UPM EP-II-9(1000): NGZ pers. obs.). The lateral face of the articular is convex for the articulation with the surangular (Fig. 16G). The posterior edge of the element is strongly elongate and tapered posteriorly (as in *Plutoniosaurus bedengensis* Efimov, 1997, and unlike any other ophthalmosaurid).

Axial skeleton. The axial skeleton has no marked difference from that of the type species.

Pectoral girdle and forelimb. The right scapula is nearly complete and 225 mm long proximodistally. It is similar to that of the type species in having a slightly curved, strap-like shaft, an oval cross section, and a small acromial process (Fig. 17K–P). The glenoid contribution is equal in size to the coracoid facet (Fig. 17K, N–P).

The coracoid (Fig. 17J) is poorly preserved and similar to that of the type species, having a lateral scapular facet markedly smaller than and poorly demarcated from the glenoid contribution.

The right forelimb is exceptionally preserved (Fig. 17A). The humerus is slender relative to that of any other ophthalmosaurid, having a proportionally small and isometric proximal end and slender diaphysis. Distally it bears three distal facets: the posterodistally deflected ulnar facet, the distally facing radial facet, and a small, circular and excavated anterior facet for an accessory epipodial element (Fig. 17A, C, E). The distal end of the humerus is slightly anteroposteriorly broader than proximal, resembling the basal thunnosaurian condition. The proximal articular surface is isometric, as long anteroposteriorly as it is tall dorsoventrally, and has an irregularly humpy surface (Fig. 17F). The dorsal trochanter is broken and cannot be described. The deltopectoral crest is more pronounced than that of the type species; it is slightly plate-like, but still relatively small compared to the condition in derived platypterygiines, e.g. *Platypterygius australis* (Wade 1984).

The ulna is hexagonal in dorsal view and a proximodistally shortened element. Distally it bears three nearly equal-sized facets for the intermedium, ulnare and pisiform. The posterior edge of the ulna bears a short facet for contact with the postaxial accessory neomorphic element, which is preserved in articulation with the right ulna (Fig. 17G–I).

The radius is hexagonal in dorsal view (Fig. 17A). Its morphology is typical of the genus and similar to the condition observed in most other Jurassic ophthalmosaurids.

The autopodial elements are tightly packed and polygonal in outline (Fig. 17A). The limb structure is typical

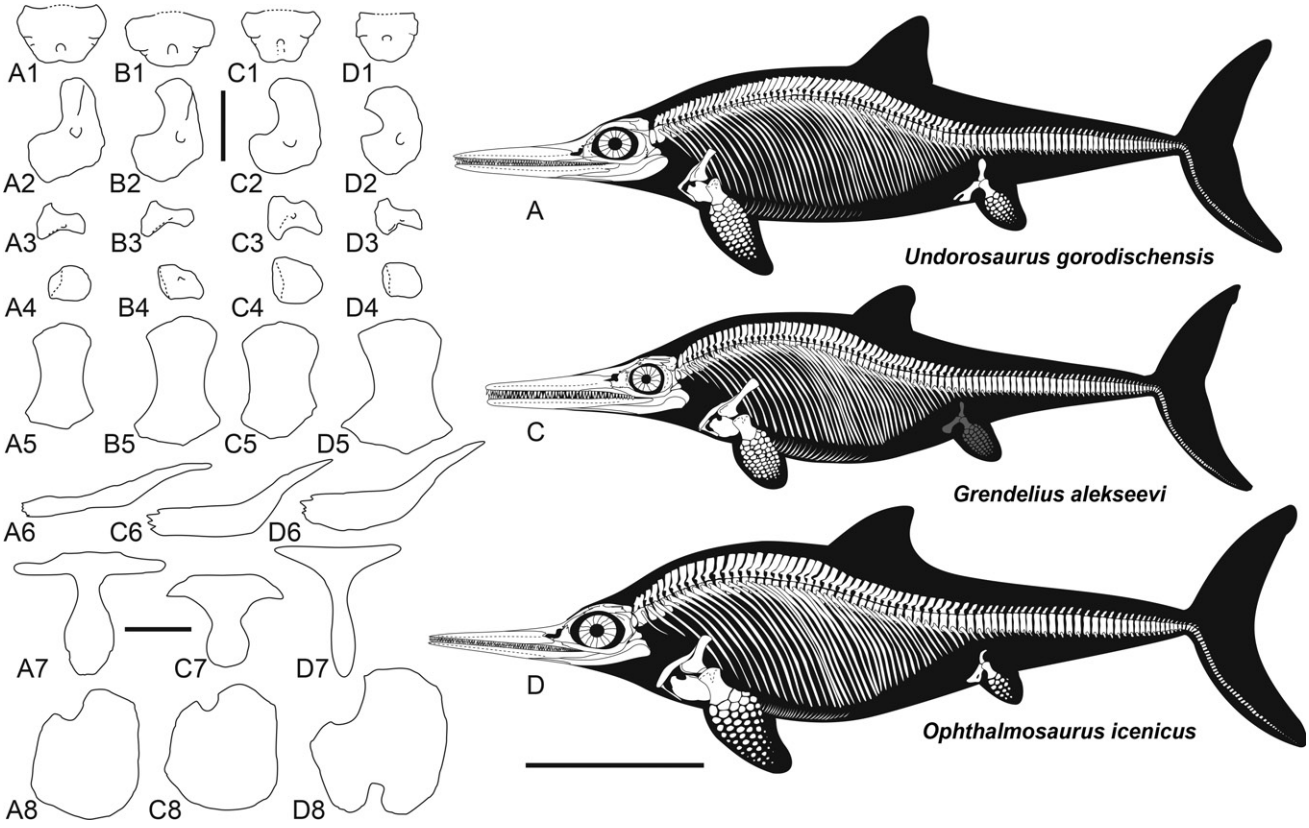

Figure 19. Skeletal reconstructions and outline drawings of selected skeletal elements of the best-known large Middle to Late Jurassic ophthalmosaurid genera *Ophthalmosaurus*, *Grendelius* and *Undorosaurus.* **A,** *Undorosaurus gorodischensis*; **B,** *Undorosaurus nessovi*; **C,** *Grendelius alekseevi*; **D,** *Ophthalmosaurus icenicus*. Compared elements are indicated with the same numbers: 1, basisphenoid; 2, quadrate; 3, stapes; 4, articular, 5, humerus; 6, clavicle; 7, interclavicle; 8, coracoid. Scale bars for skeletal elements = 10 cm; scale bar for skeletal reconstructions = 100 cm.

of the genus. The ulnare bears two nearly equal-sized distal facets for distal carpal 4 and metacarpal 5. The intermedium is proximodistally short and anteroposteriorly elongate, with an extensive distal facet for distal carpal 3, and two small distal facets for distal carpal 2 anteriorly and distal carpal 4 posteriorly. The preaxial accessory digit is well developed and as long as the other digits. It is uncertain whether the postaxial digit is absent or poorly developed, as this part of the fin is not preserved.

Phylogenetic results

Our analysis recovered six most parsimonious trees of 284 steps in length, with consistency index (CI) = 0.426 and retention index (RI) = 0.658. The strict consensus (293 steps; CI = 0.413; RI = 0.639) is well resolved; however, support for relationships within Ophthalmosauridae is low (Fig. 18).

The recovered topology is dissimilar in a number of aspects to previous analyses (i.e. Fischer *et al.* 2012 and all subsequent works based on that data set). Clade 'N' in Figure 18 (*Nannopterygius* clade) which includes *Nannopterygius enthekiodon*, *Paraophthalmosaurus saveljeviensis* and *Gengasaurus nicosiai* is recovered as the sister group to all other ophthalmosaurids. The division of Ophthalmosauridae into two distinct clades (i.e. Ophthalmosaurinae and Platypterygiinae *sensu* Fischer *et al.* 2012) is supported here; however, the composition of these clades is somewhat different from that in previous analyses (Fischer *et al.* 2012, 2016; Roberts *et al.* 2014; Delsett *et al.* 2017). Ophthalmosaurinae ('O' in Fig. 18) are recovered as including *Ophthalmosaurus* spp., *Mollesaurus periallus* and *Acamptonectes densus*, similarly to the result of Fischer *et al.* (2012).

A clade that includes *Arthropterygius chrisorum*, *Palvennia hoybergeti*, *Janusaurus lundi* and *Keilhauia nui* ('A' in Fig. 18, *Arthropterygius* clade) is recovered as the sister group to Platypterygiinae, or as a basal Platypterygiinae depending on the perception of the latter. Clade 'A' has relatively high bootstrap (58) and jackknife (67) values, thus being the best supported clade in our analysis. Similar clades were recovered by

Maxwell *et al.* (2016) and Paparella *et al.* (2017). However, contrary to their results, our analysis does not support a close relationship of this clade with '*Cryopterygius kristiansenae*' (i.e. *Undorosaurus gorodischensis* herein).

Platypterygiinae is the largest clade recovered within Ophthalmosauridae and *Undorosaurus* falls within this clade, which also comprises *Grendelius* spp., *Caypullisaurus bonapartei*, *Platypterygius* spp., *Sisteronia seeleyi*, *Maiaspondylus lindoei* and *Plutoniosaurus bedengensis*. Therefore, contrary to previous analyses (e.g. Arkhangelsky & Zverkov 2014; Roberts *et al.* 2014; Delsett *et al.* 2017; Moon 2017; Paparella *et al.* 2017), *Undorosaurus* is recovered deeply nested within Platypterygiinae as a sister taxon to the most derived platypterygiines (Fig. 18). Similarly, Motani *et al*. (2017) and Ji *et al.* (2016) recovered '*Cryopterygius kristiansenae*' as closely related to derived platypterygiines. Another interesting result is the recovery of *Leninia* as a derived platypterygiine, similar to the results of Motani *et al*. (2017) and contrary to Fischer *et al.* (2014b); however, this is still poorly substantiated considering the incompleteness of the holotype. The relationships of derived platypterygiines are still poorly resolved (Fig. 18).

Additional analyses with '*Cryopterygius kristiansenae*' PMO 214.578 and *Undorosaurus gorodischensis* UPM EP-II-20(572) coded as separate OTUs do not show any differences from the results of the main analysis (see Supplemental Fig. S3). As expected, these two OTUs form a sister clade to *U. nessovi*, further supporting the synonymy of *Cryopterygius kristiansenae* and *Undorosaurus gorodischensis*.

Discussion

Distinction of species of *Undorosaurus*

We identify four valid species of *Undorosaurus*: *Undorosaurus gorodischensis*, *U. nessovi*, *U. trautscholdi* and *U. kielanae*. Whereas two of these species are known from specimens complete enough to allow comparison of both cranial and postcranial traits, the other two are known from very scarce remains: an incomplete forelimb (SGM 1503) is the type and only specimen of *U. trautscholdi*, while for *U. kielanae* several vertebrae, an incomplete pectoral girdle, a forelimb and poor cranial remains are assigned as the type specimen (GMUL UŁ 3579-81). In this regard, the only way to compare all the species of *Undorosaurus* is to compare their forelimbs, and in particular humeri, which are known for every specimen. In general morphology, all specimens that we referred to *U. gorodischensis* have an anteroposteriorly elongated humeral proximal end of roughly oval outline (Fig. 2C, E, H, K), whereas *U. nessovi* and *U. trautscholdi* are characterized by a nearly circular outline of the humeral proximal end. Furthermore, *U. trautscholdi* has a more robust humerus than *U. nessovi*, the latter being remarkable in its slender diaphysis and proportionally long humerus (Fig. 17A–D; see also Supplemental Tables S1–S3). *Undorosaurus kielanae* is the oldest known (see Fig. 1) and smallest species of *Undorosaurus*, with a humeral length of only 118 mm. However, this could be because of the ontogenetic age of the type specimen (GMUL UŁ 3579-81). The two distal facets described for GMUL UŁ 3579-81 are possibly in this condition; however, it could be a misinterpretation, as in the case of PMO 214.578, and needs to be revised. Other cranial and postcranial remains of GMUL UŁ no. 3579-81 share characteristic features of the genus *Undorosaurus*: supranarial process of the premaxilla strongly reduced and not contacting the external naris (reinterpretation based on Tyborowski 2016, fig. 3); large robust teeth with numerous, fine enamel striations and stout roots, square in cross section; relatively reduced acromial process of the scapula; and mediolaterally compressed scapular shaft, oval in cross section (see Tyborowski 2016). Interpreting GMUL UŁ 3579-81 as a valid species of *Undorosaurus* is tentative pending personal examination of the material.

As indicated above, we consider *Cryopterygius kristiansenae* a junior subjective synonym of *Undorosaurus gorodischensis*. We could not find any feature in overlapping material between the type specimens of the two that could be used to distinguish *Cryopterygius kristiansenae* as a valid species of *Undorosaurus*. All skeletal elements overlapping in the type specimens are highly similar if not identical in both morphology (Fig. 2) and size (Supplemental Table S1). These are: dermatocranial bones including nasal, jugal, quadratojugal (see description above); basicranial elements including basioccipital, basisphenoid and stapes (although basicranial elements of PMO 214.578 are currently under study by Lene L. Delsett and therefore figures cannot be included in this contribution to make the synonymy of the two taxa more robust); and postcranial elements, especially those of the appendicular skeleton (see Fig. 2).

Being relatively well known, even when only the type specimens are considered, *Undorosaurus gorodischensis* and *U. nessovi* could be further compared using cranial characters, especially those from the occipital region of the skull. The basisphenoid of *U. gorodischensis* has anterolaterally oriented basipterygoid processes (Fig. 5A), while in *U. nessovi* the processes are oriented posterolaterally (Fig. 15A). The stapes of *U.*

gorodischensis has a peculiar teardrop-shaped medial head (Figs 5I, 6I), whereas in *U. nessovi* the stapedial head is circular in outline (Fig. 5H). Furthermore, orientation of the stapedial shaft in these species is different with respect to the stapedial head: in *U. gorodischensis* it is horizontal and in *U. nessovi* it is somewhat raised (compare Figs 5E and 15E). Quadrates in the two species could be distinguished by the size and shape of the condyle: the condyle is massive and mediolaterally broadened in *U. nessovi*, whereas in *U. gorodischensis* it is not so broad mediolaterally (compare Fig. 5V and Fig. 15L); additionally, the occipital lamella of the quadrate of *U. nessovi* appears more pronounced than that of *U. gorodischensis*. The morphology of the articular further allows distinction of *U. gorodischensis* from *U. nessovi*; in *U. gorodischensis* it is isometric in medial view, without a medial bulge, whereas in *U. nessovi* it is rhomboidal in medial view with a protruding posterior end and a pronounced bulge on the medial articular surface (compare Fig. 6F–I and Fig. 16E–G). Given all the listed differences between the two taxa, we consider them separate valid species of *Undorosaurus.*

Comparison of *Undorosaurus* with other ophthalmosaurids

Compared to contemporary ophthalmosaurids, *Undorosaurus* is more similar to *Grendelius* (Fig. 19): it has a robust rostrum, relatively small orbit and expanded postorbital region (McGowan 1976; Zverkov *et al.* 2015a). The proportions of the orbital and rostral regions of the skull of *Undorosaurus* are also similar to those of *Caypullisaurus* and most derived platypterygiines (e.g. Wade 1990; Kear 2005; Fernández 2007; Kolb & Sander 2009; Fischer 2012). *Undorosaurus* has 53 robust teeth present in each upper jaw, as in *Grendelius* and unlike *Ophthalmosaurus* (∼48) (Druckenmiller *et al.* 2012; Moon & Kirton 2016).

The external naris of *Undorosaurus* has a simple outline similar to that of *Ophthalmosaurus* (see Moon & Kirton 2016); however, its posterior portion is contributed to by the ascending process of the maxilla, but not the lacrimal as it is in *Ophthalmosaurus*, *Grendelius* and, generally speaking, all other Late Jurassic ophthalmosaurids (Zverkov *et al.* 2015a; Moon & Kirton 2016). In contrast, derived platypterygiines, such as *Platypterygius australis*, also have this condition with the ascending process of the maxilla contributing to the posterior border of the external naris and contacting the nasal dorsally (Kear 2005).

The orbital region of *Undorosaurus* is more similar to those of *Grendelius* and *Caypullisaurus* than to those of *Ophthalmosaurus* or *Janusaurus* and *Palvennia* (see Druckenmiller *et al.* 2012; Roberts *et al.* 2014; Moon & Kirton 2016): the jugal of *Undorosaurus* is robust, its suborbital bar is thick and nearly straight and the posterior process is flared as in *Grendelius*, *Caypullisaurus* and *Platypterygius* (McGowan 1976; Kear 2005; Fernández 2007; Kolb & Sander 2009). The postorbital bar of *Undorosaurus* is anteroposteriorly broad due to a pronounced lateral expansion of the jugal and quadratojugal, as in *Grendelius*, *Caypullisaurus* and *Platypterygius* (McGowan 1976; Kear 2005; Fernández 2007; Kolb & Sander 2009; Fischer 2012).

Considering its derived phylogenetic position, it is surprising that *Undorosaurus* has a squamosal, which is triangular in shape and similar to those of *Ophthalmosaurus* (Moon & Kirton 2016) and *Palvennia* (pers. obs.). However, the presence of the squamosal in certain ophthalmosaurids should be considered with great caution, as this element is very thin and poorly attached to the rest of the postorbital bar. In this regard, coding the squamosal as absent could give a misleading phylogenetic signal, as in the case of its 'absence' in *Cryopterygius kristiansenae* and *Palvennia hoybergeti* indicated by Druckenmiller *et al.* (2012) and further considered in all recent phylogenies (Roberts *et al.* 2014; Fischer *et al.* 2016; Ji *et al.* 2016; Maxwell *et al.* 2016; Delsett *et al.* 2017; Moon 2017; Paparella *et al.* 2017).

The occipital region of *Undorosaurus* also demonstrates a 'mosaic' combination of traits. The basioccipital is very similar to that of *Ophthalmosaurus* in having a reduced extracondylar area that is visible in ventral and lateral view. Surprisingly, *Plutoniosaurus bedengensis* has a very similar basioccipital with an extensive (reduced, but not extremely reduced) extracondylar area and pronounced ventral notch (pers. obs. of the holotype UPM 2/740), further calling into question the significance of an extremely reduced extracondylar area as a phylogenetic signal for platypterygiines. The stapes of *Undorosaurus* is similar to that of *Ophthalmosaurus* (see Andrews 1910; Appleby 1956; Moon & Kirton 2016): the stapedial shaft is moderately stout, unlike the slender and gracile forms in *Janusaurus*, *Palvennia* and *Acamptonectes* (Druckenmiller *et al.* 2012; Fischer *et al.* 2012; Roberts *et al.* 2014); on the other hand, it is less robust than in *Grendelius*, *Plutoniosaurus* and *Sisteronia* (Zverkov *et al.* 2015a; Fischer *et al.* 2014a; pers. obs. of *Plutoniosaurus*). A distinct difference is the stapedial facet for the opisthotic that is poorly pronounced in comparison to those of other ophthalmosaurids. The opisthotic of *Undorosaurus* has a robust and shortened paroccipital process unlike that of *Ophthalmosaurus* and *Acamptonectes* (Fischer *et al.* 2012; Moon & Kirton 2016); however, a short and robust paroccipital process is the standard condition for all other ophthalmosaurids

(see Fischer *et al.* 2014a). The columnar exoccipital occurs in stem parvipelvians (e.g. McGowan 1973; Maisch 2002) as well as in derived ophthalmosaurids, e.g. *Sveltonectes* (Fischer *et al.* 2011) and *Platypterygius* (Wade 1990, Kear 2005; Kolb & Sander 2009). In *Undorosaurus* it is clearly columnar, but not squat like those of *Acamptonectes* (Fischer *et al.* 2012) and *Grendelius* (McGowan 1976; Zverkov *et al.* 2015a).

The basisphenoid of *Undorosaurus* is remarkable for its extensive basipterygoid processes resulting in a high width-to-length ratio (1.67–1.73) that significantly exceeds the ratio of any other ophthalmosaurid: 1.5 in *Grendelius*; 1.26–1.58 in *Ophthalmosaurus* (based on the measurements of Andrews 1910); 1.26 in *Arthropterygius*; 1.37 in *Acamptonectes*; 1.3 in *Platypterygius*; and 1.2 in *Sveltonectes* and *Sisteronia* (see Supplemental Table S2; all ratios measured from figures of or calculated based on measurements from the following literature: Broili 1907; Andrews 1910; McGowan 1976; Kear 2005; Maxwell 2010; Fischer *et al.* 2011, 2012, 2014a).

The quadrate of *Undorosaurus* has a distinct L-shaped outline due to reduction of the occipital lamella, making *Undorosaurus* dissimilar to *Ophthalmosaurus* (see Andrews 1910; Moon & Kirton 2016), *Acamptonectes* (Fischer *et al.* 2012) and *Palvennia hoybergeti* (Druckenmiller *et al.* 2012) but similar to the Cretaceous platypterygiines (e.g. Broili 1907; Kear 2005; Fischer *et al.* 2014a). The marked feature of the quadrate of *Undorosaurus* is the pronounced ridge bordering the pterygoid lamella of the supratemporal; however, this feature, not reported for other ophthalmosaurids, occurs in *Plutoniosaurus bedengensis* as well (pers. obs.).

The axial skeleton of *Undorosaurus* is very similar to those of other moderate and large contemporary ophthalmosaurids. It is unlikely that an isolated centrum of *Undorosaurus* could be somehow easily distinguished from that of *Ophthalmosaurus* or *Grendelius* (Moon & Kirton 2016; NGZ pers. obs.). The clearest difference in the vertebral column of these ophthalmosaurids is vertebral count: the vertebral column of *Undorosaurus* has *c.* 52 presacral vertebra, as in *Aegirosaurus* (Bardet & Fernández 2000) and *Caypullisaurus* (Fernández 2007) and unlike *Ophthalmosaurus* (*c.* 42) and *Grendelius* (*c.* 47–50) (Zverkov *et al.* 2015a; Moon & Kirton 2016).

The appendicular skeleton of *Undorosaurus* demonstrates a number of unexpected features as well. The medial portion of the scapula of *Undorosaurus* has a relatively slight anteroposterior expansion. It appears so due to a poorly developed acromial process, unlike that of all other ophthalmosaurids (e.g. Maxwell & Kear 2010; Fischer *et al.* 2012; Moon & Kirton 2016; Zverkov *et al.* 2015a, b). Therefore, *Undorosaurus* is somewhat similar to some stem parvipelvians (e.g. McGowan & Motani 2003; Fischer *et al.* 2013). In contrast, the expanded medial portion of the scapula in *Grendelius* (see Efimov 1998; Zverkov *et al.* 2015a) is much more similar to the fan-shaped one of derived platypterygiines (e.g. Maxwell & Kear 2010; Zammit *et al.* 2010). The scapular shaft of *Undorosaurus* is mediolaterally compressed as in *Ophthalmosaurus*, *Arthropterygius*, *Janusaurus*, *Palvennia*, *Keilhauia*, *Acamptonectes* and *Sveltonectes* (Fischer *et al.* 2011, 2012; Roberts *et al.* 2014; Moon & Kirton 2016; Delsett *et al.* 2017; NGZ pers. obs.) and distinct from the thick and rod-like forms of *Grendelius* and *Platypterygius* spp. (e.g. Kolb & Sander 2009; Maxwell & Kear 2010; Zammit *et al.* 2010; Zverkov *et al.* 2015a).

The clavicles of *Undorosaurus* are unique for ophthalmosaurids, being slender and rod-like. Other ophthalmosaurids have plate-like and comparatively larger clavicles (e.g. Andrews 1910; Maxwell & Caldwell 2006b; Maxwell & Druckenmiller 2011). The most massive and robust clavicles appear to be present in ophthalmosaurids of the *Arthropterygius* clade, *Janusaurus lundi* and *Palvennia hoybergeti* (Roberts *et al.* 2014; NGZ pers. obs.).

The interclavicle of *Undorosaurus* has a markedly expanded, spatulate posterior median stem like that of *Grendelius* (Fig. 19; Efimov 1998; Zverkov *et al.* 2015a) and unlike any other ophthalmosaurid; however, compared to that of *Grendelius*, the interclavicle of *Undorosaurus* is more slender and less stocky (Fig. 19, A7, C7).

The coracoids of *Undorosaurus* are oval in outline, being slightly longer anteroposteriorly than wide mediolaterally, and mediolaterally wider at the posterior end than at the midpoint; this is very similar to those of *Grendelius* (see Fig. 19; Zverkov *et al.* 2015a). The other similarity of the coracoids of *Undorosaurus* and *Grendelius* is the poorly demarcated glenoid contribution and scapular facet (Fig. 19). The medial coracoid facet of *Undorosaurus* is not as thick as that of some Cretaceous forms (e.g. Arkhangelsky *et al.* 2008; Zammit *et al.* 2010; Fischer *et al.* 2011) but more massive than that of *Ophthalmosaurus* (Andrews 1910; Moon & Kirton 2016), *Arthropterygius* (Maxwell 2010) and *Janusaurus* (Roberts *et al.* 2014), being comparable to that of *Grendelius* (Zverkov *et al.* 2015a).

Undorosaurus gorodischensis has a relatively small forelimb similar in proportions to those of *Grendelius* spp. (Fig. 19); in contrast, the forelimbs of *Undorosaurus nessovi* are proportionally bigger and similar in relative size to those of *Ophthalmosaurus* (see Fig. 19 A5, B5, C5, D5). The forelimb of *Undorosaurus*

has five digits, as in *Grendelius*, compared with six in *Ophthalmosaurus*, *Brachypterygius* and *Aegirosaurus* (Boulenger 1904; Bardet & Fernández 2000; Moon & Kirton 2016), and more than six in *Caypullisaurus* and all Cretaceous platypterygiines for which more or less complete forelimbs are known (Broili 1907; Kuhn 1946; Efimov 1997; Fernández 1997; Maxwell & Caldwell 2006a, b; Zammit *et al.* 2010). The presence of the sixth digit anterior to the preaxial accessory digit in *Undorosaurus* is questionable; however, it is not impossible, as this condition can be also observed in the nearly contemporary *Grendelius alekseevi* (Zverkov *et al.* 2015a), indicating that the capacity to evolve more than one preaxial accessory digit became possible relatively early in the evolutionary history of platypterygiines.

The humerus of *Undorosaurus* commonly has three distal facets: ulnar and radial facets nearly equal in size, and a small (or even absent in some cases) anterior accessory facet. This condition is similar to that of most ophthalmosaurids (e.g. McGowan & Motani 2003); the most marked difference is demonstrated by ophthalmosaurids having an intermedium-humeral contact, i.e. *Brachypterygius* (Boulenger 1904; Huene 1922), *Grendelius* (McGowan 1997; Zverkov *et al.* 2015a), *Caypullisaurus* (Fernández 1997; reinterpreted *sensu* Arkhangelsky 2001b: see discussion below and Supplemental Fig. S4) and *Aegirosaurus* (Bardet & Fernández 2000). All these taxa lack a preaxial accessory facet on the humerus.

As is shown for *Undorosaurus*, the presence or absence of a preaxial accessory facet on the humerus could easily be misinterpreted when this facet is small. For example, it is traditionally considered that *Platypterygius platydactylus* has only two distal facets (e.g. McGowan 1972; Maxwell & Kear 2010; Zammit *et al.* 2010). However, it can be clearly seen from the description of Broili (1907) that the radius of *P. platydactylus* has an extensive anterior facet for the preaxial accessory element (consider that the forelimb of *P. platydactylus* was long misinterpreted as the left, and only recently was this disputed by Fischer *et al.* 2016, supplementary data, 58), and the humerus of *P. platydactylus* has a small facet anterior to the radial facet (see Broili 1907, pl. 3, fig. 15). The presence or absence of a preaxial accessory facet in *Nannopterygius* should also be considered with caution pending thorough revision of the holotype. In this regard, it is hard to compare *Undorosaurus* with other ophthalmosaurids by the presence or absence of a preaxial accessory facet. What can be said is that *Undorosaurus* differs from taxa with extensive preaxial accessory facets, comparable in size to the radial facets, such as *Arthropterygius chrisorum* (Maxwell 2010), *Maiaspondylus lindoei* (Maxwell & Caldwell 2006a; reinterpreted, see Supplemental Fig. S4) and '*Platypterygius ochevi*' (Arkhangelsky *et al.* 2008).

The humerus of *Undorosaurus* has a poorly pronounced deltopectoral crest like those of *Ophthalmosaurus*, *Arthropterygius* and *Grendelius* (Andrews 1910; Maxwell 2010; Zverkov *et al.* 2015a; Moon & Kirton 2016) and distinct from the pronounced plate-like deltopectoral crest of derived platypterygiines (e.g. Fischer *et al.* 2014a).

The forelimb structure of *Undorosaurus* is typically 'longipinnate'. It is worth mentioning that 'longipinnate' and 'latipinnate' conditions were redefined by Zverkov *et al.* (2015a) as follows: metacarpal five contacting ulnare posterodistally is the 'longipinnate' condition; metacarpal five contacting ulnare directly distally is the 'latipinnate' condition (see the description of character 89 in the Supplemental material). This should henceforth be considered more appropriate compared to the previous definition that used the contact of intermedium with distal carpals; as in such cases, the intermedium contacting equally two distal carpals will be interpreted as the 'latipinnate condition'. This does not take into consideration whether these are distal carpals 3 and 4, or distal carpals 2 and 3 as coded in, for example, '*Cryopterygius kristiansenae*', thereby resulting in a misleading signal. The intermedium of *Undorosaurus* has an extensive distal contact with distal carpal 3, and an anterodistal contact with distal carpal 2, unlike in *Ophthalmosaurus*, *Arthropterygius*, *Brachypterygius* and *Aegirosaurus* (all of which have the 'latipinnate' condition) and similar to that of the Cretaceous platypterygiines *Platypterygius platydactylus*, *P. australis*, *P. americanus*, '*P. ochevi*' and *Maiaspondylus lindoei* (Broili 1907 [re-interpreted]; Maxwell & Caldwell 2006a [re-interpreted; see Supplemental Fig. S4]; Arkhangelsky *et al.* 2008; Maxwell & Kear 2010; Zammit *et al.* 2010).

The posterior edge of the ulna of *Undorosaurus* commonly lacks perichondral ossification and contacts a postaxial accessory neomorphic element, as in *Grendelius alekseevi* and *Caypullisaurus bonapartei* (Fernández 2001; Zverkov *et al.* 2015a). The phalanges of *Undorosaurus* are rounded to polygonal in outline, not as tightly packed as in *Caypullisaurus* and other derived Cretaceous platypterygiines (McGowan 1972; Fernández 2001; McGowan & Motani 2003). However, in mature specimens of *Undorosaurus* they are more compactly arranged than in *Ophthalmosaurus* and ichthyosaurs of the *Arthropterygius* clade (see Maxwell 2010; Roberts *et al.* 2014; Moon & Kirton 2016; NGZ pers. obs.).

The pelvic girdle of *Undorosaurus* is mediolaterally compressed and anteroposteriorly wide as in *Ophthalmosaurus* (see Andrews 1910; Moon & Kirton 2016). The principal postulated difference between the *Undorosaurus* and *Ophthalmosaurus* pelves was incomplete mesial fusion of the ischium and pubis; however, as pointed out by Maisch & Matzke (2000) and later by Maisch (2010), the incomplete fusion of the pelvic bones occurs as a rare individual variation in *Ophthalmosaurus*, and indeed this condition can be observed in *Ophthalmosaurus*, e.g. NHMUK R4754 (pers. obs.). On the other hand, in *Undorosaurus* it appears more the normal condition than a deviation. It should be emphasized that the medially split ischiopubis of *Undorosaurus* is a derived autapomorphic condition rather than plesiomorphic retention.

Taxonomic framework for recovered phylogeny

Current understanding of Ophthalmosauridae Baur, 1887 defines this group either as 'the last common ancestor of *Brachypterygius* and *Ophthalmosaurus*, and all its descendants' (Motani 1999a; McGowan & Motani 2003; Ji *et al.* 2016), or as 'the last common ancestor of *Arthropterygius chrisorum* and *O. icenicus* plus all its descendants' (Fischer *et al.* 2011). The latter definition was proposed by Fischer *et al.* (2011) in order to consider *Arthropterygius* within Ophthalmosauridae; in our phylogenetic hypothesis the outlier is the *Nannopterygius* clade, recovered as the sister group to other ophthalmosaurids (Fig. 18). It is clear that these taxa (i.e. *Arthropterygius* and *Nannopterygius*) are actually more similar to other ophthalmosaurids than to basal baracromians. The recently emended definition of Ophthalmosauridae by Moon (2017, p. 20) includes "all taxa more closely related to *Ophthalmosaurus icenicus* and *Platypterygius hercynicus* than to *Stenopterygius aaleniensis* and *Chacaicosaurus cayi* [stem-based]", which we follow as it is appropriate for our results too.

It is worth emphasizing that the family Undorosauridae Efimov, 1999b cannot stand in light of the current understanding of Ophthalmosauridae. However, the authors' opinions on this issue are different. One of us, NGZ, supports the current understanding of Ophthalmosauridae, whereas VME argues that the original diagnosis of Ophthalmosauridae, proposed by Baur in 1887 (i.e. "radius, ulna, and a third bone articulating with the humerus and teeth rudimentary or absent" (Baur 1887, p. 840)) as well as the understanding of the composition of this family by earlier workers (Baur 1887; Appleby 1956) is suitable for a clade that comprises *Ophthalmosaurus*, *Mollesaurus* and *Acamptonectes* (i.e. Ophthalmosaurinae *sensu* Fischer *et al.* 2012, as interpreted here by NGZ). In this regard, VME considers this clade to be of family-level rank, representing the family Ophthalmosauridae in its original definition. Consequently, its sister clade that includes *Undorosaurus* represents the family Undorosauridae Efimov, 1999b rather than the subfamily Platypterygiinae Arkhangelsky, 2001a. The latter is more suitable for a smaller clade within Undorosauridae, comprising the most-derived Cretaceous representatives of this group (Fig. 18). Indeed, in the context of recovered phylogenetic relationships (Fig. 18), the hypothesis of Efimov (1999b) that *Undorosaurus* could be an 'ancestral form' of *Platypterygius* receives new light and provides additional support for the taxonomic context proposed by VME. It is worth mentioning that a similar taxonomic context for this group was proposed by Arkhangelsky (2001a) who identified the subfamily Platypterygiinae as including only *Platypterygius* and being within the family Undorosauridae (Arkhangelsky 2001a, p. 521). When considering derived ichthyosaurs as being represented by two families, Ophthalmosauridae and Undorosauridae, the question arises as to what to call the group that comprises these families and closely related taxa. NGZ proposes that in the case such a taxonomic context is applied, the name Ophthalmosauria, as proposed by Motani (1999a), is appropriate for this unranked clade that represents a group above the family level (Fig. 18).

Phylogenetic results, with notes on Late Jurassic ophthalmosaurid palaeobiogeography

The results of the phylogenetic analysis presented here should be considered tentative, as our work on ophthalmosaurid phylogeny is still in progress and a number of Russian ophthalmosaurids await further thorough revision.

Clade 'N', a *Nannopterygius* clade, is recovered as the sister group to all other ophthalmosaurids. Indeed, this clade is characterized by a number of primitive traits in the morphology of the skull (Characters: 12, state 0; 38 state 0; 51, state 0) and pectoral girdle (Character 69, state 1). The taxonomy and implications of this clade will be addressed elsewhere along with a thorough revision of '*Paraophthalmosaurus*' and '*Yasykovia*', which is in progress. This result is of great interest as previous phylogenies have not included *Nannopterygius* and *Paraophthalmosaurus* (cf. Moon 2017), and recovered *Arthropterygius chrisorum* as a basalmost ophthalmosaurid (Fischer *et al.* 2011 and all following works), which is not surprising considering poor scoring of the incomplete *Arthropterygius*. In fact, a number of other ophthalmosaurid taxa have been recovered at the base of Ophthalmosauridae due to a large amount of missing data e.g. *Keilhauia nui* (Delsett *et al.* 2017). A similar explanation could be proposed

for the recovery of *Undorosaurus* close to the base of Ophthalmosauridae in a number of previous analyses (Roberts *et al.* 2014; Maxwell *et al.* 2016; Delsett *et al.* 2017; Paparella *et al.* 2017). It is worth mentioning that a similar phylogenetic position of *Nannopterygius* as a sister group to other Ophthalmosauridae was recently hypothesized by Maisch (2015) but without a formal analysis.

The other important result of the analysis is the recovery of *Caypullisaurus* as more distantly related to derived platypterygiines than was previously suggested (see Fischer *et al.* 2012 and all subsequent works based on that data set). This rearrangement is mostly affected by the reinterpretation of the forefin structure of *Caypullisaurus*. The interpretation of the epipodial elements of *Caypullisaurus* by Motani (1999b) and Fernández (2001) is widely accepted, whereas the interpretation proposed by Arkhangelsky (2001b) has been neglected by most researchers. However, Arkhangelsky's interpretation is consistent with one of the most fundamental hypotheses of tetrapod limb development – the 'digital arch' hypothesis of Shubin & Alberch (1986) – whereas Motani's interpretation is in contradiction with this hypothesis (if applied, it results in a disruption at the base of the digital arch of *Caypullisaurus*) and therefore unlikely to be accepted. In fact, the only reasonable interpretation for *Caypullisaurus* is the humerus distally contacting the radius, intermedium and ulna (Supplemental Fig. S4).

Due to a very high scoring of the characters (90%), *Undorosaurus gorodischensis* finally has its place among ophthalmosaurids, and it is intriguing that *Undorosaurus* is recovered not as a basal ophthalmosaurid and not even as an ophthalmosaurine, but as a derived platypterygiine. However, against the general similarity to contemporary ophthalmosaurids, *Undorosaurus* demonstrates a number of cranial and postcranial traits that unambiguously support such results (see comparison above).

As was already discussed, many Late Jurassic ichthyosaurs had cosmopolitan distributions, and even those that are not claimed to be widespread could be shown as such after new discoveries (Zverkov *et al.* 2015a, b). 'Endemic' assemblages of Jurassic marine reptiles in certain regions (e.g. Arkhangelsky 2001a; Roberts *et al.* 2014) seem unlikely. In this regard, the palaeobiogeographical significance of our taxonomic decisions and phylogenetic results is clear.

One of the principal results of our phylogenetic analysis is the recovery of two clades that can be considered 'genera' in traditional taxonomy. These clades are the *Nannopterygius* clade (Fig. 18, 'N') and the *Arthropterygius* clade (Fig. 18, 'A'). Zverkov *et al.* (2015b) already provided some discussion of the palaeobiogeographical significance of *Arthropterigius*, and another paper on ichthyosaurs of the *Arthropterigius* clade is in preparation. The *Arthroptherygius* clade has a wide distribution that is remarkably bipolar, with at least one specimen known from the Tithonian of Argentina (Fernández & Maxwell 2012). Representatives of the *Nannopterygius* clade are known mostly from Europe (England, Italy and European Russia) and existed during the Kimmeridgian–Tithonian (Hulke 1871; Huene 1922; Arkhangelsky 1997; Moon & Kirton 2016; Paparella *et al.* 2017). It is remarkable that such a distribution is consistent with that of *Grendelius* from coeval strata (see Zverkov *et al.* 2015a), providing additional support for the close relationship of the marine reptile fauna of Eastern European seas and the Middle Russian Sea during the Kimmeridgian and early Tithonian.

Undorosaurus gorodischensis, found in the Volgian (Tithonian) of European Russia and Svalbard, supports the idea of intensive exchange of ichthyosaurs between the Middle Russian Sea and Arctic seas during the late Tithonian.

Acknowledgements

We sincerely thank Jørn H. Hurum, Lene L. Delsett, May-Liss Knudsen Funke and Bjørn Funke for their hospitality and valuable assistance during NGZ's work with the PMO collections, 27–30 September 2017. Mikhail A. Rogov (GIN) provided valuable consultations on the stratigraphy and ammonites of the Boreal Upper Jurassic. We are immensely grateful to Benjamin C. Moon (University of Bristol) for linguistic corrections and suggestions that improved the manuscript. The reviews of Aubrey J. Roberts and Benjamin C. Moon were beneficial for this work. We thank the Willi Hennig Society for their sponsorship, making TNT available for researchers free of cost. During the work on this contribution NGZ was partially supported by State Program No. 0135-2018-0035, by Program of RAS No. 17 0135-2018-0050 (Geological Institute, Russian Acad. Sci.), and by the Russian Foundation for Basic Research, Project No. 18-35-00221.

Supplemental material

Supplemental material for this article can be accessed at http://dx.doi.org/10.1080/14772019.2018.1515793.

ORCID

Nikolay G. Zverkov http://orcid.org/0000-0002-9731-1977

References

Andrews, C. W. 1910. *A descriptive catalogue of the marine reptiles of the Oxford Clay, Part I*. British Museum (Natural History), London, 205 pp, 10 pls.

Appleby, R. M. 1956. The osteology and taxonomy of the fossil reptile *Ophthalmosaurus*. *Proceedings of the Zoological Society of London*, **126**, 403–447.

Arkhangelsky, M. S. 1997. On a new ichthyosaurian genus from the Lower Volgian substage of the Saratov, Volga Region. *Paleontological Journal*, **31**, 87–90.

Arkhangelsky, M. S. 1998. On the ichthyosaurian fossils from the Volgian stage of the Saratov Region. *Paleontological Journal*, **32**, 192–196.

Arkhangelsky, M. S. 2001a. The historical sequence of Jurassic and Cretaceous ichthyosaurs. *Paleontological Journal*, **35**, 521–524.

Arkhangelsky, M. S. 2001b. On a new ichthyosaur of the genus *Otschevia* from the Volgian Stage of the Volga Region near Ulyanovsk. *Paleontological Journal*, **35**, 629–634.

Arkhangelsky, M. S. & **Zverkov, N. G.** 2014. On a new ichthyosaur of the genus *Undorosaurus*. *Proceedings of the Zoological Institute RAS*, **318**(3), 187–196.

Arkhangelsky, M. S., **Averianov, A. O.**, **Pervushov, E. M.**, **Ratnikov, V. Y.** & **Zozyrev, N. Y.** 2008. On ichthyosaur remains from the Cretaceous of the Voronezh Region. *Paleontological Journal*, **42**, 287–291.

Bardet, N. & **Fernández, M.** 2000. A new ichthyosaur from the Upper Jurassic lithographic limestones of Bavaria. *Journal of Paleontology*, **74**, 503–511.

Baur, G. 1887. Über den Ursprung der Extremitäten der Ichthyopterygia. *Jahresberichte und Mitteilungen des Oberrheinischen Geologischen Vereins*, **20**, 17–20.

Blainville, H. M. de. 1835. Description de quelques espèces de reptiles de la Californie, précédée de l'analyse d'un système général d'érpetologie et d'amphibiologie. *Nouvelles annales du Muséum d'Histoire naturelle, Paris*, **4**, 233–296.

Boulenger, G. A. 1904. On a new species of ichthyosaur from Bath. *Proceedings of the Zoological Society of London*, **1904**(1), 424–426. [Title on reprint].

Bragin, V. Yu., **Dzyuba, O. S.**, **Kazansky, A. Yu.** & **Shurygin, B. N.** 2013. New data on the magnetostratigraphy of the Jurassic–Cretaceous boundary interval, Nordvik Peninsula (northern East Siberia). *Russian Geology and Geophysics*, **54**(3), 335–348.

Broili, F. 1907. Ein neuer Ichthyosaurus aus der norddeutschen Kreide. *Palaeontographica*, **54**, 139–162.

Delsett, L. L., **Roberts, A. J.**, **Druckenmiller, P. S.** & **Hurum, J. H.** 2017. A new ophthalmosaurid (Ichthyosauria) from Svalbard, Norway, and evolution of the ichthyopterygian pelvic girdle. *PLoS ONE*, **121**(1), e0169971.

Delsett, L. L., **Novis, L. K.**, **Roberts, A. J.**, **Koevoets, M. J.**, **Hammer, Ø.**, **Druckenmiller, P. S.** & **Hurum, J. H.** 2016. The Slottsmøya marine reptile Lagerstätte: depositional environments, taphonomy and diagenesis. *Special Publication of the Geological Society, London*, **434**, 165–188.

Druckenmiller, P. S. & **Maxwell, E. E.** 2014. A Middle Jurassic (Bajocian) ophthalmosaurid (Reptilia, Ichthyosauria) from the Tuxedni Formation, Alaska and the early diversification of the clade. *Geological Magazine*, **151**, 41–48.

Druckenmiller, P. S., **Hurum, J.**, **Knutsen, E. M.** & **Nakrem, H. A.** 2012. Two new ophthalmosaurids (Reptilia: Ichthyosauria) from the Agardhfjellet Formation (Upper Jurassic: Volgian/Tithonian), Svalbard, Norway. *Norwegian Journal of Geology*, **92**, 311–339.

Efimov, V. M. 1997. A new genus of ichthyosaurs from the Late Cretaceous of the Ulyanovsk Volga Region. *Paleontological Journal*, **31**, 422–426.

Efimov, V. M. 1998. An ichthyosaur, *Otschevia pseudoscythica* gen. et sp. nov. from the Upper Jurassic strata of the Ulyanovsk region. *Paleontological Journal*, **32**, 187–191.

Efimov, V. M. 1999a. Ichthyosaurs of a new genus *Yasykovia* from the Upper Jurassic strata of European Russia. *Paleontological Journal*, **33**, 92–100.

Efimov, V. M. 1999b. A new family of ichthyosaurs, the Undorosauridae fam. nov. from the Volgian stage of the European part of Russia. *Paleontological Journal*, **33**, 174–181.

Fernández, M. S. 1997. A new ichthyosaur from the Tithonian (Late Jurassic) of the Neuquén Basin (Argentina). *Journal of Paleontology*, **71**, 479–484.

Fernández, M. S. 1999. A new ichthyosaur from the Los Molles Formation (Early Bajocian), Neuquen Basin, Argentina. *Journal of Paleontology*, **73**, 677–681.

Fernández, M. S. 2001. Dorsal or ventral? Homologies of the forefin of *Caypullisaurus* (Ichthyosauria: Ophthalmosauria). *Journal of Vertebrate Paleontology*, **21**, 515–520.

Fernández, M. S. 2003. Ophthalmosauria (Ichthyosauria) forefin from the Aalenian–Bajocian boundary of Mendoza Province, Argentina. *Journal of Vertebrate Paleontology*, **23**, 691–694.

Fernández, M. S. 2007. Redescription and phylogenetic position of *Caypullisaurus* (Ichthyosauria: Ophthalmosauridae). *Journal of Paleontology*, **81**, 368–375.

Fernández, M. S. & **Maxwell, E. E.** 2012. The genus *Arthropterygius* Maxwell (Ichthyosauria: Ophthalmosauridae) in the Late Jurassic of the Neuquén Basin, Argentina. *Geobios*, **45**, 535–540.

Fischer, V. 2012. New data on the ichthyosaur *Platypterygius hercynicus* and its implications for the validity of the genus. *Acta Palaeontologica Polonica*, **57**, 123–134.

Fischer, V., **Bardet, N.**, **Guiomar, M.** & **Godefroit, P.** 2014a. High diversity in Cretaceous ichthyosaurs from Europe prior to their extinction. *PLoS ONE*, **9**(1), e84709. doi.org/10.1371/journal.pone.0084709

Fischer, V., **Masure, E.**, **Arkhangelsky, M. S.** & **Godefroit, P.** 2011. A new Barremian (Early Cretaceous) ichthyosaur from Western Russia. *Journal of Vertebrate Paleontology*, **31**, 1010–1025.

Fischer V., **Arkhangelsky, M. S.**, **Uspensky, G. N.**, **Stenshin, I. M.** & **Godefroit, P.** 2014b. A new Lower Cretaceous ichthyosaur from Russia reveals skull shape

conservatism within Ophthalmosaurinae. *Geological Magazine*, **151**, 60–70.

Fischer, V., **Bardet, N.**, **Benson, R. B. J.**, **Arkhangelsky, M. S.** & **Friedman, M.** 2016. Extinction of fish-shaped marine reptiles associated with reduced evolutionary rates and global environmental volatility. *Nature Communications*, **7**, 1–11.

Fischer, V., **Appleby, R. M.**, **Naish, D.**, **Liston, J.**, **Riding, J. B.**, **Brindley, S.** & **Godefroit, P.** 2013. A basal thunnosaurian from Iraq reveals disparate phylogenetic origins for Cretaceous ichthyosaurs. *Biology Letters*, **9**, 20130021.

Fischer, V., **Maisch, M. W.**, **Naish, D.**, **Kosma, R.**, **Liston, J.**, **Joger, U.**, **Krüger, F.J.**, **Pardo Pérez, J.**, **Tainsh, J.** & **Appleby, R. M.** 2012. New ophthalmosaurid ichthyosaurs from the European Lower Cretaceous demonstrate extensive ichthyosaur survival across the Jurassic–Cretaceous boundary. *PLoS ONE*, **7**(1), e29234. doi.org/10.1371/journal.pone.0029234

Goloboff, P. & **Catalano, S.** 2016. TNT, version 1.5, with a full implementation of phylogenetic morphometrics. *Cladistics*, **32**, 221–238. doi.org/10.1111/cla.12160

Houša, V., **Pruner P.**, **Zakharov, V. A. Kostak**, **M.**, **Chadima, M.**, **Rogov, M. A.**, **Šlechta, S.** & **Mazuch, M.** 2007. Boreal-Tethyan correlation of the Jurassic–Cretaceous boundary interval by magneto- and biostratigraphy. *Stratigraphy and Geological Correlation*, **15**(3), 63–75.

Huene, F. von. 1922. *Die Ichthyosaurier des Lias und ihre Zusammenhänge*. *Monographien zur Geologie und Paläontologie, 1*. Verlag von Gebrüder Borntraeger, Berlin, 114 pp.

Hulke, J. W. 1871. Note on an *Ichthyosaurus* (*I. enthekiodon*) from Kimmeridge Bay, Dorset. *Quarterly Journal of the Geological Society of London*, **27**, 440–441.

Ji, C., **Jiang, D.-Y.**, **Motani, R.**, **Rieppel, O.**, **Hao, W.-C.** & **Sun, Z.-Y.** 2016. Phylogeny of the Ichthyopterygia incorporating recent discoveries from South China. *Journal of Vertebrate Paleontology*, **36**, e1025956.

Kear, B. P. 2005. Cranial morphology of *Platypterygius longmani* Wade, 1990 (Reptilia: Ichthyosauria) from the Lower Cretaceous of Australia. *Zoological Journal of the Linnean Society*, **145**, 583–622.

Kiselev, D. N., **Rogov, M. A.** & **Zakharov, V. A.** 2018. The *Volgidiscus singularis* Zone of the terminal horizons of the Volgian Stage of European Russia and its significance for interregional correlation and paleogeography. *Stratigraphy and Geological Correlation*, **26**(2), 206–233.

Kolb, C. & **Sander, P. M.** 2009. Redescription of the ichthyosaur *Platypterygius hercynicus* (Kuhn 1946) from the Lower Cretaceous of Salzgitter (Lower Saxony, Germany). *Palaeontographica, Abteilung A*, **288**, 151–192.

Kuhn, O. 1946. Ein skelett von *Ichthyosaurus hercynicus* n. sp. aus dem Aptien von Gitter. *Berichte der Naturforschenden Gesellschaft Bamb*, **29**, 69–82.

Maisch, M. W. 2002. A braincase of *Temnodontosaurus nuertingensis* cf. *trigonodon* (von Theodori, 1843) (Ichthyosauria) from the Lower Jurassic of Germany. *Geologica et Palaeontologica*, **36**, 115–122.

Maisch, M. W. 2010. Phylogeny, systematics, and origin of the Ichthyosauria – the state of the art. *Palaeodiversity*, **3**, 151–214.

Maisch, M.W. 2015. Fischechsen (Ichthyosauria). Pp. 422–430 in G. Arratia, H.-P. Schultze, H. Tischlinger & G. Viohl (eds) *Solnhofen – Ein Fenster in die Jurazeit*, *Volume 2*. Verlag Dr. Friedrich Pfeil, Munich.

Maisch, M. W. & **Matzke, A. T.** 2000.The Ichthyosauria. *Stuttgarter Beiträge zur Naturkde*. *Serie B (Geologie und Paläontologie)*, **298**, 1–159.

Maisch, M. W. & **Matzke, A. T.** 2006. The braincase of *Phantomosaurus neubigi* (Sander, 1997), an unusual ichthyosaur from the Middle Triassic of Germany. *Journal of Vertebrate Paleontology*, **26**, 598–607.

Martja, B. & **Wierzbowski, A.** 2016. Ammonites and ammonite stratigraphy of the uppermost Jurassic (Tithonian) of the Owadów–Brzezinki quarry (central Poland). *Volumina Jurassica*, **14**(1), 65–122.

Maxwell, E. 2010. Generic reassignment of an ichthyosaur from the Queen Elizabeth Islands, northwest territories, Canada. *Journal of Vertebrate Paleontology*, **30**, 403–415.

Maxwell, E. & **Caldwell, M. W.** 2006a. A new genus of ichthyosaur from the Lower Cretaceous of Western Canada. *Palaeontology*, **49**, 1043–1052.

Maxwell, E. & **Caldwell, M. W.** 2006b. Evidence for a second species of the ichthyosaur *Platypterygius* in North America: a new record from the Loon River Formation (Lower Cretaceous) of northwestern Canada. *Canadian Journal of Earth Sciences*, **43**, 1291–1295.

Maxwell, E. & **Druckenmiller, P.** 2011. A small ichthyosaur from the Clearwater Formation (Alberta, Canada) and a discussion of the taxonomic utility of the pectoral girdle. *Paläontologie Zeitschrift*, **85**, 457–463.

Maxwell, E. & **Kear, B. P.** 2010. Postcranial anatomy of *Platypterygius americanus* (Reptilia: Ichthyosauria) from the Cretaceous of Wyoming. *Journal of Vertebrate Paleontology*, **30**, 1059–1068.

Maxwell, E., **Fernández,, M. S.** & **Schoch, R. R.** 2012. First diagnostic marine reptile remains from the Aalenian (Middle Jurassic): a new ichthyosaur from southwestern Germany. *PLoS ONE*, **7**(8), e41692. doi.org/10.1371/journal.pone.0041692

Maxwell, E., **Dick, D.**, **Padilla, S.** & **Parra, M. L.** 2016. A new ophthalmosaurid ichthyosaur from the Early Cretaceous of Colombia. *Papers in Palaeontology*, **2**, 59–70.

McGowan, C. 1972. The systematics of Cretaceous ichthyosaurs with particular reference to the material from North America. *Contributions to Geology, University of Wyoming*, **11**, 9–29.

McGowan, C. 1973. The cranial morphology of the Lower Liassic latipinnate ichthyosaurs of England. *Bulletin of the British Museum (Natural History), Geology Series*, **24**, 1–109.

McGowan, C. 1976. The description and phenetic relationships of a new ichthyosaur genus from the Upper Jurassic of England. *Canadian Journal of Earth Sciences*, **13**, 668–683.

McGowan, C. 1997. The taxonomic status of the late Jurassic ichthyosaur *Grendelius mordax*: a preliminary report. *Journal of Vertebrate Palaeontology*, **17**, 428–430.

McGowan, C. & **Motani, R.** 2003. *Handbook of paleoherpetology, Part 8, Ichthyopterygia*. Verlag Dr. Friedrich Pfeil, Munich, 175 pp.

Mesezhnikov, M. S. 1984. *Kimeridzhskiy i Volzhskiy Yarusy Severa SSSR*. Nedra, Moscow, 224 pp. [In Russian.]

Moon, B. C. 2017. A new phylogeny of ichthyosaurs (Reptilia: Diapsida). *Journal of Systematic Palaeontology*, doi: 10.1080/14772019.2017.1394922

Moon, B. C. & **Kirton, A. M.** 2016. *Ichthyosaurs of the British Middle and Upper Jurassic. Part 1, Ophthalmosaurus. Monograph of the Palaeontographical Society, London*, 84 pp., 30 pls.

Motani, R. 1999a. Phylogeny of the Ichthyopterygia. *Journal of Vertebrate Paleontology*, **19**, 473–496.

Motani, R. 1999b. On the evolution and homologies of ichthyopterygian forefins. *Journal of Vertebrate Paleontology*, **19**, 28–41.

Motani, R., **Jiang, D.-Y.**, **Tintori, A.**, **Ji, C.** & **Huang, J.-D.** 2017. Pre- versus post-mass extinction divergence of Mesozoic marine reptiles dictated by time-scale dependence of evolutionary rates. *Proceedings of the Royal Society, Series B*, **284**, 20170241.

Paparella, I., **Maxwell, E.**, **Cipriani, A.**, **Roncacè, S.** & **Caldwell, M.** 2017. The first ophthalmosaurid ichthyosaur from the Upper Jurassic of the Umbrian–Marchean Apennines (Marche, Central Italy). *Geological Magazine*, **154**, 837–858.

Roberts, A. J., **Druckenmiller, P. S.**, **Saetre, G. P.** & **Hurum, J. H.** 2014. A new upper Jurassic ophthalmosaurid ichthyosaur from the Slottsmøya Member, Agardhfjellet Formation of Central Spitsbergen. *PLoS ONE*, **9**(8), e103152. doi.org/10.1371/journal.pone.0103152

Rogov, M. A. 2010a. A precise ammonite biostratigraphy through the Kimmeridgian-Volgian boundary beds in the Gorodischi section (Middle Volga area, Russia), and the base of the Volgian Stage in its type area. *Volumina Jurassica*, **8**, 103–130.

Rogov, M. A. 2010b. New data on ammonites and stratigraphy of the Volgian stage in Spitzbergen. *Stratigraphy and Geological Correlation*, **18**, 505–531.

Rogov, M. A. 2017. Ammonites and infrazonal stratigraphy of the Kimmeridgian and Volgian Stages of southern part of the Moscow Syneclise. *Transactions of the Geological Institute*, **615**, 7–160.

Rogov, M. A. & **Zakharov, V.** 2009. Ammonite- and bivalve-based biostratigraphy and Panboreal correlation of the Volgian Stage. *Science in China, Series D, Earth Sciences*, **52**(12), 1890–1909.

Sander, P. M. 2000. Ichthyosauria: their diversity, distribution, and phylogeny. *Paläontologische Zeitschrift*, **74**, 1–35.

Sasonova, I. G. & **Sasonov, N. T.** 1967. [Palaeogeography of the Russian Platform during Jurassic and Cretaceous period]. *Trudy VNIGNI*, **62**, 260 pp. [In Russian.]

Shubin, N. H. & **Alberch, P.** 1986. A morphogenetic approach to the origin and basic organization of the tetrapod limb. *Evolutionary Biology*, **20**, 319–387.

Storrs G.W., **Arkhangel'skii M.S.** and **Efimov V.M.** 2000. Mesozoic marine reptiles of Russia and other former Soviet republics. Pp. 187–210 in M. . Benton, M. A. Shishkin, D. M. Unwin & E. N. Kurochkin (eds) *The age of dinosaurs in Russia and Mongolia*. Cambridge University Press, Cambridge.

Tyborowski, D. 2016. A new ophthalmosaurid ichthyosaur from the Late Jurassic of Owadów-Brzezinki Quarry, Poland. *Acta Palaeontologica Polonica*, **61**, 791–803.

Wade, M. 1984. *Platypterygius australis*, an Australian Cretaceous ichthyosaur. Lethaia, **17**, 99–113.

Wade, M. 1990. A review of the Australian Cretaceous longipinnate ichthyosaur *Platypterygius* (Ichthyosauria, Ichthyopterygia). *Memoirs of the Queensland Museum*, **28**, 115–137.

Zammit, M., **Norris, R. M.** & **Kear, B. P.** 2010. The Australian Cretaceous ichthyosaur *Platypterygius australis*: a description and review of postcranial remains. *Journal of Vertebrate Paleontology*, **30**, 1726–1735.

Zverkov, N. G., **Arkhangelsky, M. S.** & **Stenshin, I. M.** 2015a. A review of Russian Upper Jurassic ichthyosaurs with an intermedium/humeral contact: reassessing *Grendelius* McGowan, 1976. *Proceedings of the Zoological Institute RAS*, **319**, 558–588.

Zverkov, N. G., **Arkhangelsky, M. S.**, **Pardo Perez, J. M.** & **Beznosov, P. A.** 2015b. On the Upper Jurassic ichthyosaur remains from the Russian North. *Proceedings of the Zoological Institute RAS*, **319**, 81–97.